Carbon Quantum Dots: Synthesis, Structure, Properties, and Catalytic Applications for Organic Synthesis

Pradeep Kumar Yadav [1] , Subhash Chandra [2], Vivek Kumar [3], Deepak Kumar [4] and Syed Hadi Hasan [3,*]

1   Department of Chemistry, Jagatpur P.G. College, Varanasi 221301, India
2   Department of Chemistry, Bappa Sri Narain Vocational P.G. College, Lucknow 226001, India
3   Nano Material Research Laboratory, Department of Chemistry, Indian Institute of Technology (BHU), Varanasi 221005, India
4   Department of Chemistry, Chhadami Lal Jain P.G. College, Firozabad 283203, India
*   Correspondence: shhasan.apc@itbhu.ac.in; Tel.: +91-9839089919

Abstract: Carbon quantum dots (CQDs), also known as carbon dots (CDs), are novel zero-dimensional fluorescent carbon-based nanomaterials. CQDs have attracted enormous attention around the world because of their excellent optical properties as well as water solubility, biocompatibility, low toxicity, eco-friendliness, and simple synthesis routes. CQDs have numerous applications in bioimaging, biosensing, chemical sensing, nanomedicine, solar cells, drug delivery, and light-emitting diodes. In this review paper, the structure of CQDs, their physical and chemical properties, their synthesis approach, and their application as a catalyst in the synthesis of multisubstituted 4H pyran, in azide-alkyne cycloadditions, in the degradation of levofloxacin, in the selective oxidation of alcohols to aldehydes, in the removal of Rhodamine B, as H-bond catalysis in Aldol condensations, in cyclohexane oxidation, in intrinsic peroxidase-mimetic enzyme activity, in the selective oxidation of amines and alcohols, and in the ring opening of epoxides are discussed. Finally, we also discuss the future challenges in this research field. We hope this review paper will open a new channel for the application of CQDs as a catalyst in organic synthesis.

Keywords: carbon quantum dots; synthetic methods; fluorescence; optical properties; catalyst

1. Introduction

Recently, carbon-based nanomaterials such as graphene [1], fullerenes [2], nanodiamonds [3], carbon nanotubes (CNTs) [4], and carbon quantum dots (CQDs) have attracted great attention because of their distinctive structural dimensions, as well as their outstanding chemical and physical properties [5]. It was found that the preparation and separation of nanodiamonds are complicated, while other nanomaterials such as graphene, fullerenes, and CNTs do not display good water solubility and also do not exhibit strong fluorescence in the visible region. These limitations prevent their applications in different areas [6]. Although semiconductor quantum dots (SQDs) exhibit good fluorescence properties, because of the presence of heavy metals, they are toxic in nature. This prevents their biological applicationin biosensors, bio-imaging, and drug delivery. In contrast, fluorescent CQDs are nontoxic and, thus, have attracted enormous interest over other carbon-based nanomaterials [7]. Xu et al. in 2004 accidentally discovered CQDs using gel electrophoresis during the purification of single-walled carbon nanotubes [8]. However, the name CQDs was given by Sun et al. in 2006 during the synthesis of carbon nanomaterials of different sizes [9]. Subsequently, CQDs became rising stars among various carbon-based nanoparticles and are considered an extremely precious asset of nanotechnology. CQDs are also known as carbon nano-lights because of their strong luminescence properties [10]. CQDs have attractive features such as ease of synthesis, good water solubility, high photostability, high photoresponse, low cytotoxicity, facile surface functionalization,

good catalysis properties, and tunable excitation–emission [11–17]. Due to these characteristic properties, CQDs are widely utilized in photovoltaic devices, medical diagnosis, sensing, drug delivery, catalysts, photocatalysis, optronic devices, bio-imaging, laser, single electron transistors, solar cells, and LEDs [18–29]. However, very few reports have been investigated regarding the application of CQDs as a catalyst in photochemical water splitting [30] the preparation of substituted 4H pyran with indole moieties [31], azide-alkyne cycloadditions [32], the degradation of levofloxacin [33], the selective oxidation of alcohols to aldehydes [34], the removal of Rhodamine B [35], the selective oxidation of amines and imine [36], high-efficiency cyclohexane oxidation [37], H-bond catalysis in Aldol condensations [38], intrinsic peroxidase-mimetic enzyme activity [39], and the ring opening of epoxides [40]. In this review paper, we explain the synthetic approach, structure, optical properties, and applications of CQDs as a catalyst. Finally, we also discuss their future prospects.

2. Synthesis Approach

Since the discovery of carbon quantum dots (CQDs), several convenient, cost-effective, size-controlled, and large-scale production approaches have been developed. For the synthesis of CQDs, two general categories, top-down and bottom-up, approaches are utilized (Figure 1). Even though CQDs synthesis is facile, there are definite challenges related to their synthesis, such as an aggregation of nanomaterials, the tuning of surface properties, and controlling the size and uniformity [41]. To adjust the functional groups present on the surface and achieve better CQDs performance, post-treatment can be conducted in both approaches. Quantum yields (QYs) of CQDs can be enhanced after surface passivation, which eliminates the emissive traps from the surface. CQDs doped with heteroatoms (N and P) or metals such as Au or Mg improve solubility and electrical conductivity [42]. Even though for the synthesis of CQDs, both the top-down and bottom-up approaches have been used, the environmentally and cost-effective bottom-up approach is most commonly used [43].
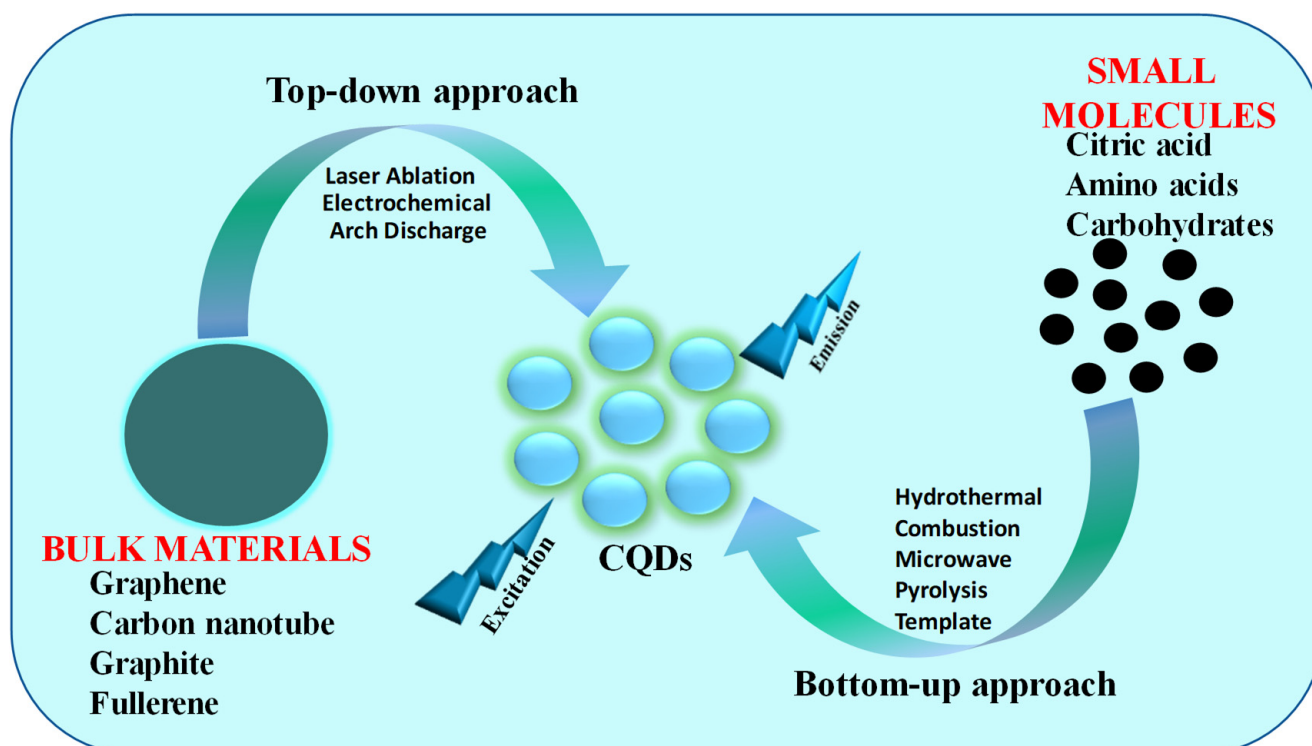

Figure 1. The typical approaches for the synthesis of CQDs.

2.1. Top-Down Approach

In a top-down approach, the larger carbon resources such as carbon nanotubes, fullerene, graphite, graphene, carbon soot, activated carbon, etc., are broken down into smaller constituents with the help of different techniques such as laser ablation and electrochemical and arch discharge [28,44–47]. Carbon structures with sp^2 hybridization that lack efficient energy gaps or band gaps are commonly used as starting materials for top-down processes. Although the top-down approach is extremely helpful and suitable for microsystem industries, it has some limitations, such as the fact that pure nanomaterials cannot be obtained from the large carbon precursor; their purification is costly and also unable to accurately control the morphology and size distribution of CQDs [48].

2.1.1. Laser Ablation Method

Sun and co-workers in 2006 first reported a laser ablation technique. In this technique, the CQDs are synthesized by irradiating a target surface with a high-energy laser pulse [9]. Recently, Li et al. synthesized ultra-small CQDs with uniform sizes by using the laser ablation method. They utilized fluorescent CQDs for cell imaging applications [49]. Cui and co-workers have also synthesized homogeneous CQDs by an ultrafast, highly efficient dual-beam pulsed laser ablation method for bio-imaging applications along with high QYs [50]. Buendia and co-workers also used laser ablation techniques to synthesize fluorescent CQDs for cell labeling [51]. The CQDs synthesized by this technique are usually non-fluorescent in nature, have heterogeneity in size, and have low quantum yield, which influences different potential applications of CQDs. Therefore, to increase the fluorescence properties and quantum yield, pre-treatments such as surface passivation (doping) and oxidation are required.

2.1.2. Electrochemical Method

The electrochemical method was first described by Zhou and coworkers in 2007. They used tetra-butyl ammonium perchlorate solution as the electrolyte to fabricate the first blue luminescent CQDs from multiwall carbon nanotubes (CNTs) [52]. In this method, larger carbon precursors are cut down into smaller parts by electrochemical oxidation in the presence of a reference electrode. Zhao et al. prepared fluorescent carbon nanomaterial by electrochemical oxidation with the help of a graphite rod as a working electrode [53]. Subsequently, Zheng and colleagues developed water soluble CQDs with tunable luminescence using graphite as an electrode material and buffering the pH with phosphate [54]. Using the oxidation method, Deng and coworkers synthesized the CQDs from low-molecular-weight alcohol. According to them, the most straightforward and convenient way to create CQDs is to conduct it under ambient pressure and temperature [55]. Hou and colleagues manufactured bright blue emitting CQDs in 2015 by treating urea and sodium citrate electrochemically in de-ionized water [56]. The electrochemical method has a few benefits; for example, it requires no surface passivation, is low cost, and has a simple purification process [42]. However, the limitation of this method is that for the synthesis of CQDs, it allows only a few little molecular precursors and has a tedious purification process. Therefore, it is the least frequently used technique [41].

2.1.3. Arch Discharge Method

Fluorescent carbon quantum dots were first discovered by Xu and coworkers accidentally during the separation and purification of a single-wall carbon nanotube by the arch discharge method. In this process, nitric acid was used as an oxidizing agent to oxidize arch ash, which formed the different functional groups on the surface, due to which aqueous solubility increased. The QYs obtained were 1.66% at a 366 nm excitation wavelength [8]. An additional experiment demonstrated that the surface of CQDs was attached to hydrophilic carboxyl groups. In the discharge process, carbon particles of different sizes are produced. CQDs obtained using this method are highly water soluble, having a wide distribution of particle sizes. Furthermore, an electronic flash method was used to separate fluorescent

nanomaterials from neat carbon nanostructures and carbon nanostructures oxidized with nitric acid [57,58]. Zhang et al. synthesized CQDs with up-conversion fluorescence using arc-synthesized carbon by-products, and Hamid Delavariet al. synthesized CQDs by arc discharge in water [59,60]. However, CQDs synthesized by this technique have some impurities that are difficult to eliminate because of their complex composition [28].

2.2. Bottom-Up Approach

In a bottom-up approach, the smaller carbon resources such as amino acids, polymers, carbohydrates, and waste materials combine to form CQDs by a variety of techniques such as hydrothermal/solvothermal, combustion, pyrolysis, and microwave irradiation. In this method, the size and structure of CQDs depend on a variety of factors such as solvent, precursor molecular structures, and conditions of the reaction (temperature, pressure, reaction time, etc.). The conditions of the reaction are necessary, since they influence the reactants and the extremely casual nucleation and escalation procedure of CQDs. This approach strengthens the material chemistry because of its ease of operation, lower cost, and easier implementation for production in a large scale [61].

The precursor used for the synthesis of CQDs may be both chemical and biological, i.e., natural. The chemical precursors include glucose, sucrose, citric acid, lactic acid, ascorbic acid, glycerol, ethylene glycol, etc. [62–68]. The natural sources include Artocarpous lakoocha seeds, rice husks, Azadirachta indica leaves, pomelo peel, the latex of Ficus benghalensis, aloe vera, etc. (Figure 2) [69–72].
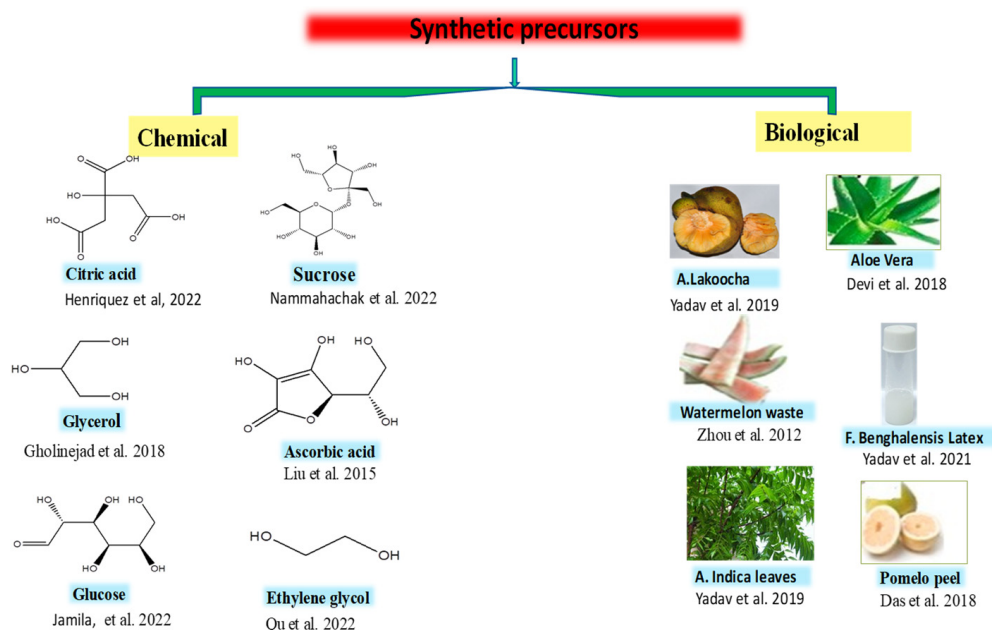
Figure 2. Chemical and biological precursors utilized for the synthesis of CQDs [61–72].

2.2.1. Hydrothermal Method

The hydrothermal method was first reported by Zhang et al., for the synthesis of CQDs from the precursor L-ascorbic acid (carbon source) without any chemical action or other surface passivation. The average size of the synthesized CQDs was ~2 nm, and the QY obtained was 6.79%. They utilized four different solvents (water, ethyl acetate, acetone, and ethanol) for the synthesis of bright blue emission CQDs and observed that the water soluble CQDs were very stable at room temperature over 6 months. Additionally, the fluorescence intensity of CQDs was stable in a wide pH range and highly ionic salt conditions (2 M NaCl) [73]. In the hydrothermal process, the precursor molecules are dissolved in water, set aside in a Teflon-lined stainless steel autoclave, and placed in the hydrothermal chamber at high temperature and pressure for a few hours [66].The precursor

molecules utilized for the synthesis include proteins, polymers, amino acids, polyols, glucose, some wastes, and natural products [13,74]. In recent years, the hydrothermal method has attracted great attention around the world because of its single step, ease of operation, nontoxicity, low cost, and ecofriendliness. CQDs prepared from the hydrothermal treatment have a range of beneficial properties, such as being highly homogeneous, watersoluble, monodispersed, and photostable, having salt tolerance and a controlled particle size, and exhibiting an elevated QY with no surface passivation. Similar to the hydrothermal method, for the synthesis of CQDs, a solvothermal method is also utilized using ammonia, alcohol, and other organic and inorganic solvents as a substitute for water [63,75–77].

2.2.2. Combustion Method

In 2007, Liu et al. first reported the combustion method to synthesize CQDs. This method involves oxidative acid treatments which aggregate smaller carbon resources into CQDs, enhance the aqueous solubility, and control the fluorescence properties. Liu and coworkers explained that candle ashes were obtained by partial combustion of a candle with aluminum foil and refluxing it in nitric acid solution. When the candle ashes were dissolved in a neutral medium followed by centrifugation and a dialysis method, the pure CQDs were obtained [78]. The CQDs synthesized by the combustion method had low QY but displayed good fluorescence without doping [70].

2.2.3. Pyrolysis Method

The pyrolysis method is the thermal decomposition of the precursor at an elevated temperature (typically over 430 °C) and under pressure in the absence of oxygen. Additionally, the carbon precursor cleavages into nanoscale colloidal particles in the presence of an alkali and strong acid concentration as a catalyst. The advantageous properties of this method include practicability, repeatability, and simplicity, as well as having a high QY. However, it is challenging to separate small precursors from raw materials.

In 2009, Liu et al. first described a novel method for the preparation of CQDs through pyrolysis using resol (as a carbon source) and surfactant-modified silica spheres. The synthesized CQDs exhibited blue fluorescence and were amorphous, with sizes ranging from 1.5 to 2.5 nm, and the QY obtained was 14.7%. Moreover, the CQDs were stable in a broad pH range (pH 5–9) [79]. After that, several investigations were carried out for the preparation of CQDs using the pyrolysis method. Pan et al., in 2010, synthesized extremely blue fluorescent CQDs from ethylenediamine-tetraacetic acid (EDTA) salts using the pyrolysis method. The average size of the synthesized CQDs was 6 nm. The quantum yield (QY) obtained was 40.6% [80]. With the help of the pyrolysis of citric acid at 180 °C, Martindale and coworkers (in 2015) synthesized fluorescent CQDs with an average size of 6 nm, and at the excitation of 360 nm, the calculated QY was 2.3% [81]. Rong and coworkers in 2017 also prepared fluorescent N-CQDs by the pyrolysis of citric acid and guanidinium chloride without organic solvent, acid, alkali, or further modification and passivation, resulting in N-CQDs with a size of 2.2 nm and a QY of 19.2%. They utilized N-CQDs intensively in the detection of metal-ion (Fe^{3+}) and in bio-imaging [82]. Lately, several CQDs were synthesized using the pyrolysis method and utilized in different fields [41,83,84].

2.2.4. Microwave Irradiation Method

Microwave synthesis is a faster and cost-effective method for the synthesis of CQDs via microwave heating. Compared to other techniques, this is a simple and convenient method because it requires less time for the synthesis of CQDs, with an improved quantum yield. Zhu et al. first synthesized fluorescent CQDs under the microwave (500W) by heating poly (ethylene glycol) (PEG-200) and saccharide for 2–10 min [48]. This method is rapid, novel, green, and energy efficient in synthesizing CQDs. However, there are some limitations, such as difficulty in the separation procedure and purification, and that non-uniform particle sizes of CQDs restrict their prospective applications [85,86]. Recently,

various investigations were carried out for the preparation of CQDs using microwave irradiation, utilizing them for different applications [87–91].

2.2.5. Template Method

Bourlinos and coworkers first synthesized fluorescent CQDs using the template method [92]. The template method involves two steps: (i) The preparation of CQDs in the appropriate template or silicon sphere by calcinations. (ii) The etching process occurs to eliminate the supporting materials. Some advantageous properties of the template method are that it is straightforward, the equipment is easily obtainable, it is suitable for the surface passivation of CQDs, it prevents the particles from agglomerating, and it controls the size of CQDs. The disadvantageous property of the template method is the difficulty in the separation of the CQDs from the template, which may affect the purity, particle size, fluorescence property, and QY.

3. Structure of CQDs

Tang et al. reported that CQDs have core–shell structures which are either amorphous (mixed sp^2/sp^3) or graphitic crystalline (sp^2), depending upon the extent of the occurrence of sp^2 carbon in the core [93]. Graphitic crystalline (sp^2) cores were reported by several researchers [94–96]. The size of cores is very small (2–3 nm), with a characteristic lattice spacing of ~0.2 nm [97]. The cores are categorized depending on the technique utilized for the synthesis and the precursors used, as well as other synthetic parameters (such as duration, temperature, pH, etc.) [98]. Generally, the graphitization (sp^2) structure is obtained at over 300 °C reaction temperatures, while amorphous cores are obtained at lower temperatures, unless sp^2/sp^3-hybridized C is present in the precursor [99]. To determine the core structure of CQDs, various instrumental techniques such as Transmission Electron Microscopy (TEM) or High Resolution (HR) TEM, Scanning Electron Microscopy (SEM), Raman spectroscopy, and X-ray diffraction (XRD) are utilized. To measure the size and morphology of the CQDs, TEM or SEM are carried out [100]. The selected area electron diffraction (SAED) patterns reveal the amorphous or crystalline nature of CQDs [101]. The XRD pattern also determines the crystal structure of CQDs. The broad peak at 2θ 23° indicates the amorphous nature of CQD, while the occurrence of two broad peaks at 2θ 25° and 44° specifies a low-graphitic carbon structure analogous to (002) and (100) diffraction [102]. The general structure and presence of different functional groups on the surface of CQDs are determined using Fourier transform infrared (FT-IR) spectroscopy, X-ray photoelectron spectroscopy (XPS), elemental analysis (EA), and nuclear magnetic resonance (NMR) [103,104]. Using nitrogen sorption analysis, the surface area of the carbon nanoparticles is calculated [103]. To decide the optical properties and qualitative information regarding the presence of C=C and C=O in CQDs, UV-Vis absorption spectroscopy is carried out [105]. To determine the positive or negative charge on the surface of CQDs and the extent of the electrostatic interaction between them, zeta potential is conceded [106,107].

Figure 3 is the typical structure of carbon quantum dots (CQDs), which reveals the presence of different functional groups (such as carbonyl, carboxyl, hydroxyl, amino, etc.) on the surface of CQDs. The presence of these functional groups was confirmed by instrumental techniques such as FTIR and XPS [108].
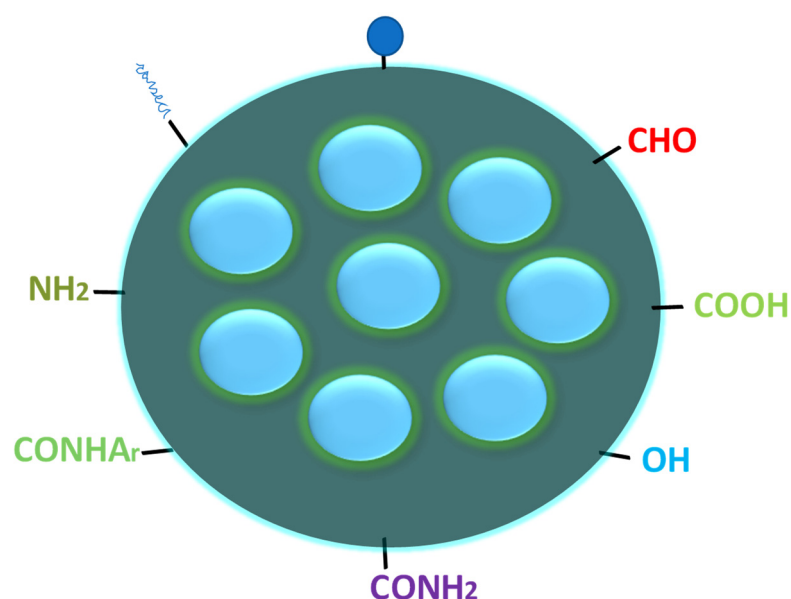
Figure 3. Typical structure of CQDs with different functional groups on the surface.

4. Optical Properties of Carbon Quantum Dots (CQDs)

4.1. Absorbance

CQDs generally exhibit two absorption bands in the visible region around 280 nm and 350 nm, alongside a tail broadly in the UV region. Hu et al. reported that an absorption band at 280 nm is due to a pi-pi* (π-π*) transition of a C=C bond, and the one at 350 nm is due to an n-π* transition of the C=O bond [109]. Figure 4 is the typical UV-visible absorption spectrum of fluorescent CQDs. The absorption properties of CQDs can be influenced by surface modification or surface passivation [110–113]. Depending on the raw precursor and synthesis methodology, the positions of these absorption bands are different to some extent. Doping in CQDs can also alter the absorption wavelength.
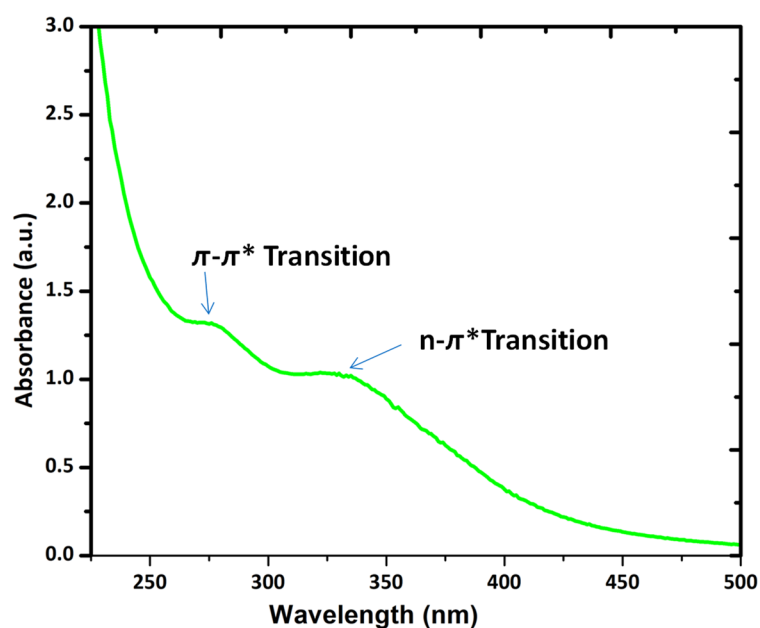
Figure 4. The UV-visible absorption spectrum of fluorescent CQDs.

The optical properties of CQDs can be customized by doping/co-doping with heteroatoms, functional groups, and surface passivation [114]. In the process of surface passivation, a slim insulating (protecting) layer of covering materials such as thiols, thionyl chloride,

spiropyrans, and oligomers (polyethylene glycol (PEG), etc.) is formed on the CQDs surface. The important functions of such types of protective layers are to shield CQDs from the adhesion of impurities and to provide stability [115]. CQDs with surface-passivating agents become extremely optically active, demonstrating considerable fluorescence from the visible to the near-IR region [116]. The quantum yields (QYs) of CQDs can also be enhanced up to 55–60% by surface passivation [114]. The absorbance of CQDs improved to longer wavelengths (350–550 nm) after surface passivation with 4,7,10-trioxa-1,13-tridecanediamine (TTDDA) [117]. Particle size is associated with the absorption wavelength. As the size of the CQDs increases, absorption wavelength also increases [118,119]. The CQDs are viable for covalent bonding with functionalizing agents [114]. Different functional groups such as amines, carboxyl, hydroxyl, carbonyl, etc., were introduced on the surface of CQDs by surface functionalization. The functionalized CQDs revealed good biocompatibility, high stability, outstanding photoreversibility, and low toxicity compared to undoped CQDs. The efficient technique to modify the CQDs absorption spectrum is doping/co-doping with heteroatoms (such as boron (B), nitrogen (N), fluorine (F), phosphorous (P), and sulfur (S)). The dopant adjusts the bandgap, electronic structure, and, consequently, the optical properties of CQDs by altering the π-π^* energy level (related through the core-sp^2 carbon system) [120]. On increasing N-dopant concentration, a gradual increase in the band gap of the CQDs from 2.2 to 2.7 eV was observed [121]. In contrast, it was also found that the doping of N in CQDs results in a reduction in size [122]. The CQDs established innovative electronic states, resulting in a reduction in the bandgap of CQDs (about ~48–57%) [123]. Zuo et al. synthesized F-doped CQDs using a hydrothermal method which exhibited higher QYs and enhanced the electron transfer and acted as a superior photocatalyst [124].

4.2. Photoluminescence

The emission of light from a substance upon the absorption of light (photon) is called photoluminescence (PL). Photoluminescence includes two types, namely fluorescence and phosphorescence. Fluorescent materials emit absorbed light from the lowest singlet excited state (S_1) to the singlet ground state (S_0). This process is very fast and has a nanosecond lifetime. The transitions that occur among two electronic states in the fluorescence process are allowed because it has the same spin multiplicity. In contrast, in phosphorescence, the transition occurs from the lowest triplet excited state (T_1) to singlet ground state (S_0), i.e., a forbidden transition occurs according to the spin selection rule.

4.2.1. Fluorescence

The fluorescence properties of CQDs have attracted great attention among researchers because of their several sensing and analytical applications. Numerous mechanisms have been reported to gain deep insight into the cause of fluorescence in CQDs [125–130]. Among them, the following two have been found more prominent. The first is that the fluorescence mechanism is due to band gaps' transitions arising from the π-conjugated domains (sp^2-hybridized), which is similar to aromatic molecules employing definite energy band gaps in favor of absorptions and emissions [131]. The second cause of fluorescence is related to the surface defects, quantum size effect, carbon core state, surface passivation/functionalization effect, and different emissive traps on the surface of CQDs [132–134].

The main reason for the surface defects in CQDs is an unsymmetrical allocation of sp^2- and sp^3-hybridized carbon atoms, and the existence of heteroatoms such as B, N, P, and S [126,135]. When this surface defect is independently incorporated into the solid host, it creates surroundings similar to aromatic molecules. These molecules can attract UV light and display various color emissions [131,136]. CQDs show two types of emission, i.e., excitation-dependent emission (tunable emission) and excitation-independent emission. The tunable emission is due to the presence of various emission sites on the surface of CQDs along with particle size distribution; because of this, most CQDs exhibit tunable emissions [137]. The excitation-independent emission is due to the extremely ordered graphitic structure of CQDs [118]. CQDs exhibit extensive and unremitting excitation

spectra which are highly photostable and have steady fluorescence, in contrast to traditional organic dye [95,138,139].

4.2.2. Phosphorescence

In CQDs, the phosphorescence property is also observed, which was first described by De et al. via dispersing CQDs to polyvinyl alcohol matrix at RT and exciting them with ultraviolet light. The maximum emission obtained was 500 nm, with an average lifetime of 380 ns at a 325 nm excitation [140]. Phosphorescence in CQDs arises when the singlet and triplet states of an aromatic carbonyl group in CQDs and polyvinyl alcohol matrix are close in energy to assist spin–orbit coupling, which increases the intersystem crossing (ISC). By using microwave synthesis, Lu et al. synthesized ultra-long phosphorescent carbon quantum dots (P-CQDs). When P-CQDs were excited at 354 nm, they displayed yellow-green phosphorescence (525 nm) for up to 9 s. They concluded that as the pH increases, the phosphorescence intensity of P-CQDs gradually decreases. The reason is that protonation dissociates the hydrogen bonds and distresses the phosphorescent sources. By introducing the tetracyclines (TCs), the phosphorescence of P-CQDs was quenched. They applied P-CQDs as biological and chemical sensing and time-resolved imaging [141]. Figure 5 is the typical excitation (black line) and emission (red line) spectrum of fluorescent CQDs.
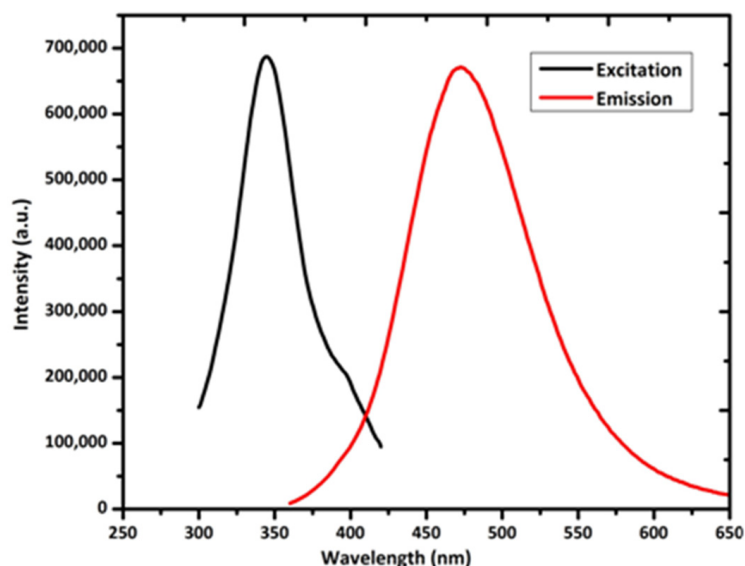

Figure 5. Excitation and emission spectrum of CQDs.

5. Application of Carbon Quantum Dots as a Catalyst

The presence of different functional groups such as -OH, -COOH, -NH$_2$, etc., on carbon quantum dots' (CQDs) surface provides vigorous coordination sites to bind with transition metal ions. The CQDs doped with multiple heteroatoms might further improve the catalytic activity by encouraging electron transfer via interior interactions. The presence of more active catalytic reaction sites offered by CQDs and favorable charge transfers during the catalytic process is also responsible for the application of CQDs as a catalyst (Figure 6) [6,142–144].
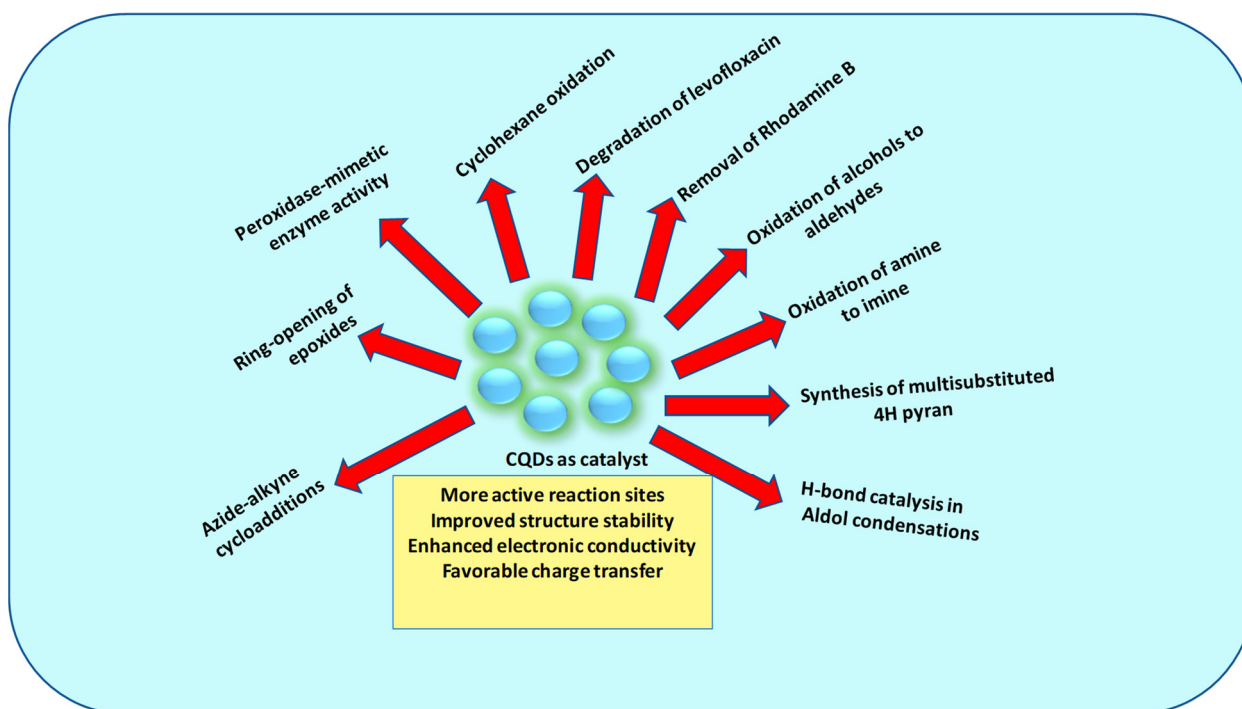
Figure 6. Catalytic applications of CQDs.

5.1. CQDs as a Catalyst for the Peroxidase-Mimetic Enzyme Activity

Natural enzymes such as peroxidase can catalyze a variety of reactions with high catalytic activity and excessive surface specificity [145]. Because of this, they are broadly utilized in different fields such as the pharmaceuticals industry, medicine, agriculture, etc. [146]. However, they possess some limitations such as high cost, short storage life, rigorous storage conditions, and poor thermal stability [147]. Therefore, to point out these limitations, carbon-based nanomaterials were found very suitable for intrinsic peroxidase-mimetic catalytic activity. Yadav et al. have synthesized fluorescent CQDs from leaf extracts of neem (*Azadirachtaindica*) by using a one-pot hydrothermal method. The as-prepared Neem-Carbon Quantum Dots (N-CQDs) exhibited peroxidase-mimetics catalytic activity in an extensive pH range for the oxidation of peroxidase substrate 3,3′,5,5′- tetramethylbenzidine (TMB) in the presence of hydrogen peroxide (H_2O_2). The peroxidase-mimetic catalytic activity of N-CQDs was confirmed by taking UV−visible absorption spectra of N-CQDs in the presence and absence of H_2O_2 with TMB in an acetate buffer. When the mixtures of TMB and N-CQDs were taken, no absorbance at 652 nm was observed, revealing no oxidation of TMB. Additionally, when the mixture of TMB and H_2O_2 reacted, a less intense peak at 652 nm was obtained, enlightening the partial oxidation of TMB with the existence of a partial blue color. Interestingly, in the presence of N-CQDs, TMB, and H_2O_2, the absorbance at 652 was found at a maximum, with the color changing from colorless to blue, revealing the complete oxidation of TMB. These results powerfully confirmed that N-CQDs act as a catalyst for peroxidase-mimetic activity. To determine the intermediate reaction, the active species trapping experiment with isopropyl alcohol (IPA) and methyl alcohol (MA) was carried out. The IPA and MA are hydroxyls radical (●OH) scavengers. When these scavengers were added to the oxidized blue-colored solution of TMB, a decrease in the absorption at 652 nm was observed, enlightening the incomplete oxidation of TMB because the IPA and MA consumed the ●OH radical. This examination specifies that in the presence of N-CQDs, the ●OH radicals were generated during a peroxidase-like catalytic reaction, which oxidized TMB via a one-electron transfer to produce a blue-colored solution. Additionally, the high surface area, small size, and presence of a negative-charge density on the N-CQDs surface were also responsible for this catalytic activity (Figure 7) [39].
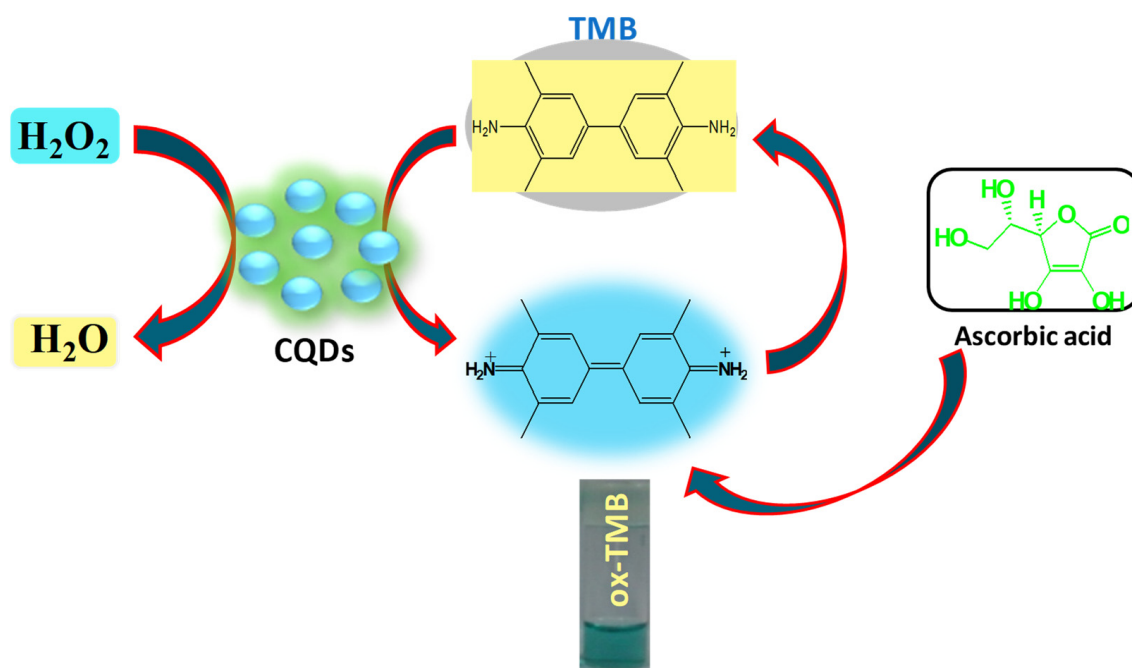
Figure 7. Showing the oxidation of TMB along with H_2O_2 in the presence of CQDs as a catalyst.

5.2. CQDs as a Catalyst for Selective Oxidation of Alcohols to Aldehydes

Aldehydes are highly demanded as a crucial intermediate for the production of an extensive range of materials, such as pesticides, toiletries, dyes, and perfumes, in the pharmaceuticals and agribusiness industries. The popular method for the synthesis of aldehydes is catalytic alcohol oxidation, but establishing an ecofriendly method with high-yield production and selectivity is still a major challenge for researchers [148–150]. Rezaie et al. developed a multifunctional tungstate-decorated CQDs base catalyst, A-CQDs/W, by using a one-pot hydrothermal technique, and utilized it for the oxidation of a variety of alcoholic substrates into analogous aldehydes with the help of H_2O_2 as an oxidant and an ultrasound effect as a green activation method. Before investigating the catalytic activity, the oxidizing potential of an amphiphilic multifunctional catalyst was examined, and they observed that A-CQDs/W were capable of oxidizing a wide range of alcoholic substances into corresponding aldehydes with 100% selectivity and above 95% yield. This achievement was because of the synergic effect among ultrasound irradiation and the suitable design of the catalyst. The proposed mechanism for this oxidation reaction firstly involves the reaction between H_2O_2 and A-CQDs/W, resulting in the production of bisperoxo tungstate, which is immobilized on A-CQDs via hydrophilic groups. This is able to diffuse into the organic alcoholic phase and trigger the oxidation reaction with the assistance of an ultrasound wave. Finally, aldehyde was fabricated after inserting the alcoholic ligand on A-CQDs/W, followed by a ligand exchange reaction [34,151,152].

5.3. CQDs as a Catalyst for Selective Oxidation of Amine to Imine

Imines are valuable for the preparation of biologically active molecules, such as oxazolidines, chiral amines, amides, nitrones, aminonitriles, and hydroxylamines. Additionally, β-lactams complexes are also synthesized using imine intermediates [153–155]. Several materials were used as a catalyst for the selective oxidation of amine to imine, but the carbon-based materials such as CQDs, mesoporous carbon, graphene oxide (GO), amorphous carbon, graphitic carbon nitride, and carbon nanotubes (CNTs) have been recognized as potential catalysts compared to conventional metal-based catalysts because of their relatively low cost and natural abundance [156–158].

Ye et al. prepared oxygen-rich carbon quantum dots (O-CQDs) from fullerenes (C_{60}) and utilized them as nanocatalysts (metal-free) for the oxidation of amines to imine with

an excellent 98% yield. The mechanism behind this catalytic oxidation reveals that the molecular oxygen and amine molecules are trapped and activated by carboxylic functional groups present on the surface of CQDs, along with the unpaired electrons, resulting in the conversion of amine. For the oxidative coupling of amine to imine, the catalytic performance of O-CQDs was further improved by heat treatment. The aerobic oxidation of amines was probably because of the occurrence of several carboxyl functional groups, which coupled with spins of π-electrons from the atoms situated at the surface of O-CQDs [36].

5.4. CQDs as a Catalyst in the Synthesis of Multisubstituted 4H Pyran with Indole Moieties

Indole scaffolds have attracted much attention among researchers because of their applications in the field of pharmacology, such as antihypertensive, antiproliferative, anticholinergic, antifungal, cardiovascular, optimal inhibitory, antibacterial, antiviral, and anticonvulsant activities [159–161]. Additionally, there are some pharmaceutically significant compounds and natural products which have anticancer, hypoglycemic, anti-inflammatory, antipyretic, and antitumor properties, and contain indole scaffolds in their structures [162,163]. 4H-pyrans are an important family of oxygen-containing heterocyclic compounds with a wide spectrum of biological properties such as antioxidant, anticoagulant, diuretic, spasmolytic, anti-anaphylactic, and anticancer activities [164,165]. Rasooll et al. synthesized a novel heterogeneous nano-catalyst from CQDs and phosphorus acid moieties by using ultrasonic irritation followed by a hydrothermal method and named it CQDs–$N(CH_2PO_3H_2)_2$. The instrumental techniques such as transmission electron microscopy (TEM), energy-dispersive X-ray (EDX) spectroscopy, X-ray diffraction (XRD), FT-IR spectroscopy, scanning electron microscopy (SEM), fluorescence, and thermogravimetric (TG) analysis were utilized to characterize this catalyst. An efficient catalyst, CQDs–N $(CH_2PO_3H_2)_2$, was effectively applied for the preparation of 2-amino-6-(2-methyl-1H-indol-3-yl)-4-phenyl-4H-pyran-3,5-dicarbonitriles, with the help of a variety of aromatic aldehydes, 3-(1H-indol3-yl)-3-oxopropanenitrile derivatives, and malononitrile. The principal advantages of this catalytic activity include fresh and mild reaction conditions, little reaction time, and the recycling of the catalyst.

The anticipated mechanism for this catalytic reaction is that, firstly, the acidic proton of CQDs–$N(CH_2PO_3H_2)_2$ activates the aldehyde group, followed by the reaction with malononitrile, and intermediate (I) is formed by the loss of one molecule of H_2O. In the next step, 3-(1Hindol-3-yl)-3-oxopropanenitrile reacts with intermediate (I) to provide intermediate (II) following tautomerization. Finally, after intramolecular cyclization, the desired product is obtained from intermediate (II) with the loss of another molecule of H_2O [31].

5.5. As a Photocatalyst for High-Efficiency Cyclohexane Oxidation

In the 21st century, the highly efficient and highly selective catalytic oxidation of cyclohexane under mild conditions is the principle objective of catalysis chemistry. Liu et al. synthesized fluorescent CQDs and gold (Au) nanoparticle composites (Au/CQDs composites). The CQDs were prepared through the electrochemical ablation method using graphite. A chemical reduction method was used to synthesize AuNPs by an aqueous solution of $HAuCl_4$ and trisodium citrate, which resulted in a pink color immediately after the addition of the $NaBH_4$ solution. When in the solution of CQDs, a HAuCl4 solution was added, and the solution turned red, revealing the formation of a composite (Au/CQDs composites). Interestingly, they utilized this composite as a tunable photocatalyst for the selective oxidation of cyclohexane to cyclohexanone with the help of an oxidant H_2O_2 (30%). The conversion efficiency was 63.8% and selectivity was over 99.9%. The mechanism involves enrichment in the absorption of light by surface plasma resonance of Au nanoparticles, the generation of active trapping oxygen species (HO·) through H_2O_2 decomposition, and interaction among CQDs and AuNPs under visible light [37].

5.6. As a Catalyst for the Removal of Rhodamine B

Preethi et al. prepared bluefluorescent CQDs from a natural carbon precursor (muskmelon peel) using a stirrer-assisted method. The synthesized CQDs were utilized as an excellent photocatalyst and a sonocatalyst for the degradation of Rhodamine B (RhB) dye. The efficiency of CQDs for the degradation of RhB is 99.11% in sunlight, with a degradation rate constant of 0.06943 min^{-1} and 83.04% in ultrasonication. These results advocate that CQDs are an efficient catalyst for the breakdown of organic dyes in wastewater. The mechanism reveals the generation of •OH radicals during active species trapping experiment. •OH was confirmed by taking terephthalic acid (TA) as a scavenger. The dye molecules adsorbed on the surface of CQDs may be oxidized by these active species, ensuing in dye degradation [35].

5.7. As a Catalyst in Azide-Alkyne Cycloadditions

Liu and coworkers synthesized yellow light-emitting bio-friendly CQDs from $Na_2[Cu(EDTA)]$ by thermolysis. Cu(I)-doped fluorescent CQDs were utilized for catalyzing the Huisgen 1,3-dipolar cycloaddition among azides and terminal alkynes, the classical example of "click chemistry". The possible mechanism behind this catalytic property using these CQDs was projected to be the UV-induced split of excitons. First of all, the escape of electrons from the CQDs occurs, resulting in the formation of holes to compete with Cu(I), and at last, Cu(I) is released from the CQDs. The high biocompatibility of this nanocatalyst was confirmed by Hep-2 cells, revealing intracellular detection [32].

5.8. As H-Bond Catalysis in Aldol Condensations

Han and coworkers synthesized CQDs by an electrochemical etching method and utilized them as efficient heterogeneous nanocatalysts for H-bond catalysis in aldol condensations. The catalytic activity was excellent (89% yields), with visible light irradiation. Highly efficient electron-accepting capabilities, novel photochemical properties, and functional hydroxyl and carboxylic groups on the surface are responsible for such soaring catalytic activities of CQDs [38]. The catalytic efficiency of CQDs was high in visible light irradiation, and almost no conversion was observed in the absence of light. The CQD-catalyzed aldol condensation was greatly influenced by solvents. Han et al. used different solvents such as ethanol, tetrahydrofuran (THF), acetone, chloroform ($CHCl_3$), and toluene. However, the highest yield (89%) was calculated when the solvent and reactant were acetone. These investigations exposed that CQDs acted as an outstanding catalyst for Aldol condensation. The mechanism revealed that the cationic or anionic intermediates were generated during catalytic reaction. The hydroxyl groups present on the CQDs edge act as extremely weak acids, which can form H-bonds with oxygenates [166,167]. Aldehydes and ketones, both reactants, were capable of forming H-bonds. They confirmed that the hydroxyl groups present on the surface of CQDs favor contact with aldehyde groups. When the reactions were carried out in the absence of a hydroxyl group, no product was obtained and free CQDs were unreactive. These results advocate that the capability of CQDs to intervene in reactions is through interfacial H-bond catalysis. In visible light irradiation, CQDs act as highly proficient electron acceptors and attract electrons from the O−H⋯O region, resulting in the development of a positive charge on hydrogen and oxygen, and the negative charge increases. This effect results in an increase in the s-character in the oxygen hybrid orbital, thereby leading to the strengthening of the O−H bond, which efficiently activates the C=O bond of the aldehyde group and accelerates the aldol condensation. Furthermore, the reaction-intermediate or transition-state species is stabilized by the enhanced O−H bonds, resulting in the highest yield of 89.4% [168,169].

5.9. As a Catalyst for the Ring Opening of Epoxides

In modern organic synthesis, acid catalytic reactions contribute a characteristic and imperative role [170]. Some carbon-based nanostructures such as sulfated-graphene/-tube/-active carbon materials have been utilized as acid catalysts in several catalytic

applications [171]. However, they possess some limitations, such as the requirement of sufficient surface functionalization, low efficiency, and complex synthesis steps [172]. As a result, the development of carbon materials-based acid catalysts with high efficiency that are light-driven or light-enhanced are still required. Keeping these in mind, Li et al. described the synthesis of CQDs based on a novel, photoswitchable solid acid catalyst. The CQDs were synthesized from a graphite rod using an electrochemical method, doped with hydrogen sulfate groups (S-CQDs). They utilized S-CQDs as light-enhanced acid catalysts, which catalyze the ring opening of epoxides in the presence of nucleophiles and solvents (methanol and other primary alcohols). The mechanism revealed that the additional protons are released from the ionization of the $-SO_3H$ group under visible light irradiation and, as a result, a stronger acid environment is offered for the opening reaction, and a higher yield as well as selectivity of the product is obtained compared to the process without light irradiation. The photoexcitation and charge separation in the CQDs create an electron-withdrawing effect from the acidic groups. The utilization of S-CQDs as visiblelight-responsive and convenient photocatalysts is a novel application of CQDs in green chemistry [40].

5.10. As a Catalyst for the Degradation of Levofloxacin

Levofloxacin (LEVO), also known as levaquin, is an important antibiotic medicine. Several bacterial infections such as pneumonia, acute bacterial sinusitis, urinary tract infection, *H. pypori*, and chronic prostatitis are treated by LEVO. It is also used to treat tuberculosis, pelvic inflammatory disease, or meningitis, along with other antibiotics [173,174]. However, the degradation of LEVO is typical. Although some techniques have been utilized for the degradation of LEVO, the degradation using CQD had not been discovered. Meng et al. synthesized CQDs@FeOOH nanoneedles for an efficient electro-catalytic degradation of LEVO. The CQDs were synthesized by a hydrothermal method from orange peels. With the help of a facile in situ growth method, the α-FeOOH was fabricated by using $Fe_2(SO4)_3$ and H_2O in 50 mL distilled water. Similarly, a CQDs@FeOOH electro-catalyst was prepared using the above method, except that 500 mL aqueous solutions of 0.5 g/L CQDs were used instead of 500 mL distilled water. By using CQDs@FeOOH, about 99.6% LEVO and 53.7% total organic carbon (TOC) could be competently removed after 60 min degradation. This high degradation performance for LEVO was due to the soaring mass transfer capability and the high % OH generation ability of the CQDs@FeOOH. Meng et al. proposed a possible LEVO degradation mechanism and also investigated the change in toxicity throughout LEVO degradation. The mechanism revealed the generation of both % OH and SO4% in LEVO degradation, but a dominant role was played by % OH. Liquid chromatography-mass spectrometry (LC-MS) results designated that the LEVO could be entirely decomposed by % OH under the de-piperazinylation, decarboxylation, and ring opening reaction. This novel work offers a proficient technique to reduce the quantity and toxicity of antibiotics in water [33].

5.11. CQDs as Electrocatalyst

CQDs are also utilized as electrocatalysts in hydrogen evolution reduction, oxygen evolution reaction, CO_2 reduction reaction and oxygen reduction reaction. The large surface area, good conductivity and fast charge transfer process of CQDs are responsible for the electrocatalytic applications [6].

6. Conclusions and Future Perspectives

The present review paper discusses the structures, synthetic methods, optical properties, and applications of CQDs as a catalyst. The structure of CQDs includes core–shell, either graphitic (sp^2) or amorphous (mixed sp^2/sp^3). CQDs are usually amorphous, having different functional groups such as amino, carboxyl, hydroxyl, etc. CQDs are synthesized by both the bottom-up and the top-down approach. The bottom-up method is better because it is ecofriendly and economically viable, but it has poor control over the size of CQDs.

In contrast, the top-down methods are expensive. For the synthesis of CQDs, chemical as well as biological precursors are used. CQDs possess admirable optical properties and have superior water solubility, low toxicity, biocompatibility, and ecofriendliness. The optical properties and QYs are essential parameters for the applications of CQDs in the field of nanomedicine, biosensing, chemical sensing, bioimaging, solar cells, drug delivery, and light-emitting diodes. In this review paper, we have focused on the applications of CQDs as a catalyst in the degradation of levofloxacin, the selective oxidation of amines and alcohols, azide-alkyne cycloadditions, the synthesis of multisubstituted 4H pyran, the selective oxidation of alcohols to aldehydes, the removal of Rhodamine B, cyclohexane oxidation, the ring opening of epoxides, and intrinsic peroxidase-mimetic enzyme activity. The mechanism suggests that the catalytic activity might be due to the presence of more active reaction sites, favorable charge transfer, improved structure stability, and enhanced electronic conductivity.

However, during the last fifteen years, several investigations have been carried out on CQDs, and numerous challenges require being resolved for the extensive adoption of CQDs. (1) It is difficult to synthesize CQDs of a desired structure and size because of the requirement of accurate control over different synthesis parameters. Therefore, to powerfully control the core structure, a manufacturing process could be developed which helps increase QYs and the large-scale production of CQDs. (2) In many research papers, it has not been reported why the fluorescence QY of doped and co-doped CQDs are high in contrast to the un-doped CQDs. Thus, in the future, it is possible to realize the basic fluorescence mechanism in doped and co-doped CQDs. (3) Most doped and co-doped CQDs emit blue fluorescence. Hence, it is challenging for the researcher to synthesize multicolor emission CQDs and utilize them in different applications in the future. (4) To broaden the spectrum of CQDs, efforts must be made, particularly in the near-IR region, so that the applications of CQDs can be widespread, such as in organic bioelectronics. (5) CQDs possess some limitations such as low reactivity, poor stability, short lifetime, etc., which prevents them from promising to be a good catalyst. Therefore, in the future, it will be possible to overcome these shortcomings.

Compared to other applications of CQDs, very few studies have been reported on the application of CQDs as a catalyst in organic synthesis. In detail, theoretical and experimental studies are required to carefully design CQD-based catalysts with attractive catalytic action and durable operation stability. The applications of CQDs as a catalyst in organic synthesis signify the flexibility of CQDs in the most unpredicted areas. It is inspiring to see the applications of CQDs in green chemistry and clean energy production. It looks obvious that the future of CQDs remains promising.

References

1. Clancy, A.; Bayazit, M.K.; Hodge, S.A.; Skipper, N.T.; Howard, C.A.; Shaffer, M.S.P. Charged Carbon Nanomaterials: Redox Chemistries of Fullerenes, Carbon Nanotubes, and Graphenes. *Chem. Rev.* **2018**, *118*, 7363–7408. [CrossRef] [PubMed]
2. Lin, H.-S.; Jeon, I.; Xiang, R.; Seo, S.; Lee, J.-W.; Li, C.; Pal, A.; Manzhos, S.; Goorsky, M.S.; Yang, Y.; et al. Achieving high efficiency in solution-processed perovskite solar cells using C60/C70 mixed fullerenes. *ACS Appl. Mater. Interfaces* **2018**, *46*, 39590–39598. [CrossRef] [PubMed]
3. Georgakilas, V.; Perman, J.A.; Tucek, J.; Zboril, R. Broad Family of Carbon Nanoallotropes: Classification, Chemistry, and Applications of Fullerenes, Carbon Dots, Nanotubes, Graphene, Nanodiamonds, and Combined Superstructures. *Chem. Rev.* **2015**, *115*, 4744–4822. [CrossRef] [PubMed]
4. Rao, R.; Pint, C.L.; Islam, A.E.; Weatherup, R.S.; Hofmann, S.; Meshot, E.R.; Wu, F.; Zhou, C.; Dee, N.; Amama, P.B.; et al. Carbon nanotubes and related nanomaterials: Critical advances and challenges for synthesis toward mainstream commercial applica-tions. *ACS Nano* **2018**, *12*, 11756–11784. [CrossRef]
5. Patel, K.D.; Singh, R.K.; Kim, H.W. Carbon-based nanomaterials as an emerging platform for theranostics. *Materials Horizons* **2019**, *3*, 434–469. [CrossRef]
6. Wang, X.; Feng, Y.; Dong, P.; Huang, J. A Mini Review on Carbon Quantum Dots: Preparation, Properties, and Electrocatalytic Application. *Front. Chem.* **2019**, *7*, 671. [CrossRef]
7. Zuo, J.; Tao, J.; Zhao, X.; Xiong, X.; Xiao, S.; Zhu, Z. Preparation and application of fluorescent carbon dots. *J. Nanomater.* **2015**, *2015*, 787862. [CrossRef]
8. Xu, X.; Ray, R.; Gu, Y.; Ploehn, H.J.; Gearheart, L.; Raker, K.; Scrivens, W.A. Electrophoretic Analysis and Purification of Fluorescent Single-Walled Carbon Nanotube Fragments. *J. Am. Chem. Soc.* **2004**, *126*, 12736–12737. [CrossRef]
9. Sun, Y.-P.; Zhou, B.; Lin, Y.; Wang, W.; Fernando, K.S.; Pathak, P.; Meziani, M.J.; Harruff, B.A.; Wang, X.; Wang, H. Quantum-Sized Carbon Dots for Bright and Colorful Photoluminescence. *J. Am. Chem. Soc.* **2006**, *128*, 7756–7757. [CrossRef]
10. Ahmad, F.; Khan, A.M. Carbon quantum dots: Nanolights. *Int. J. Petrochem. Sci. Eng.* **2017**, *2*, 247–250. [CrossRef]
11. Yang, S.; Sun, J.; Li, X.; Zhou, W.; Wang, Z.; He, P.; Ding, G.; Xie, X.; Kang, Z.; Jiang, M. Large-scale fabrication of heavy doped carbon quantum dots with tunable-photoluminescence and sensitive fluorescence detection. *J. Mater. Chem. A* **2014**, *2*, 8660–8667. [CrossRef]
12. Guo, H.; Liu, Z.; Shen, X.; Wang, L. One-Pot Synthesis of Orange Emissive Carbon Quantum Dots for All-Type High Color Rendering Index White Light-Emitting Diodes. *ACS Sustain. Chem. Eng.* **2022**, *10*, 8289–8296. [CrossRef]
13. Toma, E.E.; Stoian, G.; Cojocaru, B.; Parvulescu, V.I.; Coman, S.M. ZnO/CQDs Nanocomposites for Visible Light Photodegradation of Organic Pollutants. *Catalysts* **2022**, *12*, 952. [CrossRef]
14. Subedi, S.; Rella, A.K.; Trung, L.G.; Kumar, V.; Kang, S.-W. Electrically Switchable Anisometric Carbon Quantum Dots Exhibiting Linearly Polarized Photoluminescence: Syntheses, Anisotropic Properties, and Facile Control of Uniaxial Orientation. *ACS Nano* **2022**, *16*, 6480–6492. [CrossRef]
15. Gu, L.; Zhang, J.; Yang, G.; Tang, Y.; Zhang, X.; Huang, X.; Zhai, W.; Fodjo, E.K.; Kong, C. Green preparation of carbon quantum dots with wolfberry as on-off-on nanosensors for the detection of Fe3+ and l-ascorbic acid. *Food Chem.* **2022**, *376*, 131898. [CrossRef]
16. Chen, Y.; Xue, B. A review on quantum dots modified g-C3N4-based photocatalysts with improved photocatalytic activity. *Catalysts* **2020**, *1*, 142. [CrossRef]
17. Parya, E.; Rhim, J.-W. Pectin/carbon quantum dots fluorescent film with ultraviolet blocking property through light conversion. *Colloids Surf. B Biointerfaces* **2022**, *219*, 112804.
18. Ajayan, P.M.; Zhou, O.Z. Applications of carbon nanotubes. *Carbon Nanotub.* **2001**, *80*, 391–425.
19. Baptista, F.R.; Belhout, S.A.; Giordani, S.; Quinn, S.J. Recent developments in carbon nanomaterial sensors. *Chem. Soc. Rev.* **2015**, *44*, 4433–4453. [CrossRef]
20. Chen, D.; Tang, L.; Li, J. Graphene-based materials in electrochemistry. *Chem. Soc. Rev.* **2010**, *39*, 3157–3180. [CrossRef]
21. Cayuela, A.; Benítez-Martínez, S.; Soriano, M.L. Carbon nanotools as sorbents and sensors of nanosized objects: The third way of analytical nanoscience and nanotechnology. *TrAC Trends Anal. Chem.* **2016**, *84*, 172–180. [CrossRef]
22. Pardo, J.; Peng, Z.; Leblanc, R.M. Cancer Targeting and Drug Delivery Using Carbon-Based Quantum Dots and Nanotubes. *Molecules* **2018**, *23*, 378. [CrossRef] [PubMed]
23. Sahar, T.; Abnous, K.; Taghdisi, S.M.; Ramezani, M.; Alibolandi, M. Hybrid car-bon-based materials for gene delivery in cancer therapy. *J. Control Release* **2020**, *318*, 158–175.
24. Mingjun, C.; Cao, Y.; Zhu, Y.; Peng, W.; Li, Y.; Zhang, F.; Xia, Q.; Fan, X. Oxidation-Modulated CQDs Derived from Covalent Organic Frameworks as Enhanced Fluorescence Sensors for the Detection of Chromium (VI) and Ascorbic Acid. *Ind. Eng. Chem. Res.* **2022**, *31*, 11484–11493.
25. Murali, G.; Kwon, B.; Kang, H.; Modigunta, J.K.R.; Park, S.; Lee, S.; Lee, H.; Park, Y.H.; Kim, J.; Park, S.Y.; et al. Hematoporphyrin Photosensitizer-Linked Carbon Quantum Dots for Photodynamic Therapy of Cancer Cells. *ACS Appl. Nano Mater.* **2022**, *5*, 4376–4385. [CrossRef]
26. Li, P.; Yu, M.; Ke, X.; Gong, X.; Li, Z.; Xing, X. Cytocompatible Amphipathic Carbon Quantum Dots as Potent Membrane-Active Antibacterial Agents with Low Drug Resistance and Effective Inhibition of Biofilm Formation. *ACS Appl. Bio Mater.* **2022**, *5*, 3290–3299. [CrossRef]

27. Wu, Y.; Qin, D.; Luo, Z.; Meng, S.; Mo, G.; Jiang, X.; Deng, B. High Quantum Yield Boron and Nitrogen Codoped Carbon Quantum Dots with Red/Purple Emissions for Ratiometric Fluorescent IO_4^- Sensing and Cell Imaging. *ACS Sustain. Chem. Eng.* **2022**, *10*, 5195–5202. [CrossRef]

28. Kaur, A.; Pandey, K.; Kaur, R.; Vashishat, N.; Kaur, M. Nanocomposites of Carbon Quantum Dots and Graphene Quantum Dots: Environmental Applications as Sensors. *Chemosensors* **2022**, *10*, 367. [CrossRef]

29. Sharma, V.; Vishal, V.; Chandan, G.; Bhatia, A.; Chakrabarti, S.; Bera, M. Green, sustainable, and economical synthesis of fluorescent nitrogen-doped carbon quantum dots for applications in optical displays and light-emitting diodes. *Mater. Today Sustain.* **2022**, *19*, 100184. [CrossRef]

30. Wang, Y.; Chen, D.; Zhang, J.; Balogun, M.T.; Wang, P.; Tong, Y.; Huang, Y. Charge Relays via Dual Carbon-Actions on Nanostructured $BiVO_4$ for High Performance Photoelectrochemical Water Splitting. *Adv. Funct. Mater.* **2022**, *32*, 2112738. [CrossRef]

31. Rasooll, M.M.; Zarei, M.; Zolfigol, M.A.; Sepehrmansourie, H.; Omidi, A.; Hasani, M.; Gu, Y. Novel nano-architectured carbon quantum dots (CQDs) with phosphorous acid tags as an efficient catalyst for the synthesis of multisubstituted 4*H*-pyran with indole moieties under mild conditions. *RSC Adv.* **2021**, *11*, 25995–26007. [CrossRef]

32. Liu, Z.X.; Bin Chen, B.; Liu, M.L.; Zou, H.Y.; Huang, C.Z. Cu(i)-Doped carbon quantum dots with zigzag edge structures for highly efficient catalysis of azide–alkyne cycloadditions. *Green Chem.* **2017**, *19*, 1494–1498. [CrossRef]

33. Fanqing, M.; Wang, Y.; Chen, Z.; Hu, J.; Lu, G.; Ma, W. Synthesis of CQDs@ FeOOH nanoneedles with abundant active edges for efficient electro-catalytic degradation of levofloxacin: Degradation mechanism and toxicity assessment. *Appl. Catal. B Environ.* **2021**, *282*, 119597.

34. Rezaei, A.; Mohammadi, Y.; Ramazani, A.; Zheng, H. Ultrasound-assisted pseudohomogeneous tungstate catalyst for selective oxidation of alcohols to aldehydes. *Sci. Rep.* **2022**, *12*, 3367. [CrossRef]

35. Preethi, M.; Viswanathan, C.; Ponpandian, N. A metal-free, dual catalyst for the removal of Rhodamine B using novel carbon quantum dots from muskmelon peel under sunlight and ultrasonication: A green way to clean the environment. *J. Photochem. Photobiol. A Chem.* **2022**, *426*, 113765. [CrossRef]

36. Ye, J.; Ni, K.; Liu, J.; Chen, G.; Ikram, M.; Zhu, Y. Oxygen-Rich Carbon Quantum Dots as Catalysts for Selective Oxidation of Amines and Alcohols. *Chemcatchem* **2017**, *10*, 259–265. [CrossRef]

37. Ruihua, L.; Huang, H.; Li, H.; Liu, Y.; Zhong, J.; Li, Y.; Zhang, S.; Kang, Z. Metalnanopar-ticle/carbon quantum dot composite as a photocatalyst for high-efficiency cyclohexane oxidation. *ACS Catal.* **2014**, *1*, 328–336.

38. Han, Y.; Huang, H.; Zhang, H.; Liu, Y.; Han, X.; Liu, R.; Li, H.; Kang, Z. Carbon Quantum Dots with Photoenhanced Hydrogen-Bond Catalytic Activity in Aldol Condensations. *ACS Catal.* **2014**, *4*, 781–787. [CrossRef]

39. Pradeep Kumar, Y.; Singh, V.K.; Chandra, S.; Bano, D.; Kumar, V.; Talat, M.; Hasan, S.H. Green synthesis of fluorescent carbon quantum dots from azadirachtaindica leaves and their peroxidase-mimetic ac-tivity for the detection of H2O2 and ascorbic acid in common fresh fruits. *ACS Biomater. Sci. Eng.* **2018**, *2*, 623–632.

40. Li, H.; Sun, C.; Ali, M.; Zhou, F.; Zhang, X.; MacFarlane, D.R. Sulfated Carbon Quantum Dots as Efficient Visible-Light Switchable Acid Catalysts for Room-Temperature Ring-Opening Reactions. *Angew. Chem.* **2015**, *127*, 8540–8544. [CrossRef]

41. Wang, Y.; Hu, A. Carbon quantum dots: Synthesis, properties and applications. *J. Mater. Chem. C* **2014**, *34*, 6921–6939. [CrossRef]

42. Sofia, P.; Palomares, E.; Martinez-Ferrero, E. Graphene and carbon quantum dot-based materials in pho-tovoltaic devices: From synthesis to applications. *Nanomaterials* **2016**, *6*, 157.

43. Chae, A.Y.; Choi, S.J.; Paoprasert, N.P.; Park, S.Y.; In, I. Microwave-assisted synthesis of fuorescent carbon quantum dots from an A2/B3 monomer set. *RSC Adv.* **2017**, *7*, 12663–12669. [CrossRef]

44. Liu, Y.; Huang, H.; Cao, W.; Mao, B.; Liu, Y.; Kang, Z. Advances in carbon dots: From the perspective of traditional quantum dots. *Mater. Chem. Front.* **2020**, *4*, 1586–1613. [CrossRef]

45. Li, H.; Xu, Y.; Zhao, L.; Ding, J.; Chen, M.; Chen, G.; Li, Y.; Ding, L. Synthesis of tiny carbon dots with high quantum yield using multi-walled carbon nanotubes as support for selective "turn-off-on" detection of rutin and Al3+. *Carbon* **2018**, *143*, 391–401. [CrossRef]

46. Zhao, M.; Zhang, J.; Xiao, H.; Hu, T.; Jia, J.; Wu, H. Facile *in situ* synthesis of a carbon quantum dot/graphene heterostructure as an efficient metal-free electrocatalyst for overall water splitting. *Chem. Commun.* **2019**, *55*, 1635–1638. [CrossRef]

47. Yuan, F.; Su, W.; Gao, F. Monolayer 2D polymeric fullerene: A new member of the carbon material family. *Chem* **2022**, *8*, 2079–2081. [CrossRef]

48. Zhu, H.; Wang, X.; Li, Y.; Wang, Z.; Yang, F.; Yang, X. Microwave synthesis of fluorescent carbon nanoparticles with electrochemi-luminescence properties. *Chem. Commun.* **2009**, *34*, 5118–5120. [CrossRef]

49. Li, H.; Zhang, Y.; Ding, J.; Wu, T.; Cai, S.; Zhang, W.; Cai, R.; Chen, C.; Yang, R. Synthesis of carbon quantum dots for application of alleviating amyloid-β mediated neurotoxicity. *Colloids Surfaces B Biointerfaces* **2022**, *212*, 112373. [CrossRef]

50. Cui, L.; Ren, X.; Wang, J.; Sun, M. Synthesis of homogeneous carbon quantum dots by ultrafast dual-beam pulsed laser ablation for bioimaging. *Mater. Today Nano* **2020**, *12*, 100091. [CrossRef]

51. Doñate-Buendía, C.; Fernández-Alonso, M.; Lancis, J.; Mínguez-Vega, G. Pulsed laser ablation in liq-uids for the production of gold nanoparticles and carbon quantum dots: From plasmonic to fluorescence and cell labelling. *J. Phys. Conf. Ser.* **2020**, *1537*, 012013. [CrossRef]

52. Jigang, Z.; Booker, C.; Li, R.; Zhou, X.; Sham, T.-K.; Sun, X.; Ding, Z. An electro-chemical avenue to blue luminescent nanocrystals from multiwalled carbon nanotubes (MWCNTs). *J. Am. Chem. Soc.* **2007**, *4*, 744–745.

53. Zhao, Q.-L.; Zhang, Z.-L.; Huang, B.-H.; Peng, J.; Zhang, M.; Pang, D.-W. Facile preparation of low cytotoxicity fluorescent carbon nanocrystals by electrooxidation of graphite. *Chem. Commun.* **2008**, *41*, 5116–5118. [CrossRef]

54. Zheng, L.; Chi, Y.; Dong, Y.; Lin, J.; Wang, B. Electrochemiluminescence of Water-Soluble Carbon Nanocrystals Released Electrochemically from Graphite. *J. Am. Chem. Soc.* **2009**, *131*, 4564–4565. [CrossRef]

55. Deng, J.; Lu, Q.; Mi, N.; Li, H.; Liu, M.; Xu, M.; Tan, L.; Xie, Q.; Zhang, Y.; Yao, S. Electrochemical Synthesis of Carbon Nanodots Directly from Alcohols. *Chem. A Eur. J.* **2014**, *20*, 4993–4999. [CrossRef]

56. Hou, Y.; Lu, Q.; Deng, J.; Li, H.; Zhang, Y. One-pot electrochemical synthesis of functionalized fluorescent carbon dots and their selective sensing for mercury ion. *Anal. Chim. Acta* **2015**, *866*, 6974. [CrossRef]

57. Bottini, M.; Tautz, L.; Huynh, H.; Monosov, E.; Bottini, N.; Dawson, M.I.; Bellucci, S.; Mustelin, T. Covalent decoration of multi-walled carbon nanotubes with silica nanoparticles. *Chem. Commun.* **2004**, *6*, 758–760. [CrossRef]

58. Michelsen, H.A.; Colket, M.B.; Bengtsson, P.-E.; D'anna, A.; Desgroux, P.; Haynes, B.S.; Miller, J.H.; Nathan, G.J.; Pitsch, H.; Wang, H. A review of terminology used to describe soot formation and evo-lution under combustion and pyrolytic conditions. *ACS Nano* **2020**, *10*, 12470–12490. [CrossRef]

59. Su, Y.; Xie, M.; Lu, X.; Wei, H.; Geng, H.; Yang, Z.; Zhang, Y. Facile synthesis and photoelectric properties of carbon dots with upconversion fluorescence using arc-synthesized carbon by-products. *RSC Adv.* **2013**, *4*, 4839–4842. [CrossRef]

60. Biazar, N.; Poursalehi, R.; Delavari, H. Optical and structural properties of carbon dots/TiO2 nanostructures prepared via DC arc discharge in liquid. *IP Conf. Proc.* **2018**, *1920*, 020033.

61. Wang, L.; Ruan, F.; Lv, T.; Liu, Y.; Deng, D.; Zhao, S.; Wang, H.; Xu, S. One step synthesis of Al/N co-doped carbon nanoparticles with enhanced photoluminescence. *J. Lumin.* **2015**, *158*, 1–5. [CrossRef]

62. Inderbir, S.; Arora, R.; Dhiman, H.; Pahwa, R. Carbon quantum dots: Synthesis, characterization and biomedical applications. *Turk. J. Pharm. Sci.* **2018**, *2*, 219–230.

63. Qu, Y.; Li, X.; Zhang, H.; Huang, R.; Qi, W.; Su, R.; He, Z. Controllable synthesis of a sponge-like Z-scheme N, S-CQDs/Bi2MoO6@ TiO2 film with enhanced photocatalytic and antimicrobial activity under visi-ble/NIR light irradiation. *J. Hazard. Mater.* **2022**, *429*, 128310. [CrossRef] [PubMed]

64. Kaixin, C.; Zhu, Q.; Qi, L.; Guo, M.; Gao, W.; Gao, Q. Synthesis and Properties of Nitro-gen-Doped Carbon Quantum Dots Using Lactic Acid as Carbon Source. *Materials* **2022**, *15*, 466.

65. Henriquez, G.; Ahlawat, J.; Fairman, R.; Narayan, M. Citric Acid-Derived Carbon Quantum Dots Attenuate Paraquat-Induced Neuronal Compromise In Vitro and In Vivo. *ACS Chem. Neurosci.* **2022**, *13*, 2399–2409. [CrossRef]

66. Nammahachak, N.; Aup-Ngoen, K.K.; Asanithi, P.; Horpratum, M.; Chuangchote, S.; Ratanaphan, S.; Surareungchai, W. Hydrothermal synthesis of carbon quantum dots with size tunability *via* heterogeneous nucleation. *RSC Adv.* **2022**, *12*, 31729–31733. [CrossRef]

67. Jamila, G.S.; Sajjad, S.; Leghari, S.A.K.; Kallio, T.; Flox, C. Glucose derived carbon quantum dots on tungstate-titanate nanocom-posite for hydrogen energy evolution and solar light catalysis. *J. Nanostruct. Chem.* **2021**, *12*, 611–623. [CrossRef]

68. Qiu, Y.; Li, D.; Li, Y.; Ma, X.; Li, J. Green carbon quantum dots from sustainable lignocellulosic biomass and its application in the detection of Fe3+. *Cellulose* **2021**, *29*, 367–378. [CrossRef]

69. Aayushi, K.; Maity, B.; Basu, S. Rice Husk-Derived Carbon Quantum Dots-Based Dual-Mode Nano-probe for Selective and Sensitive Detection of Fe3+ and Fluoroquinolones. *ACS Biomater. Sci. Eng.* **2022**, *11*, 4764–4776.

70. El-Brolsy, H.M.E.M.; Hanafy, N.A.N.; El-Kemary, M.A. Fighting Non-Small Lung Cancer Cells Using Optimal Functionalization of Targeted Carbon Quantum Dots Derived from Natural Sources Might Provide Potential Therapeutic and Cancer Bio Image Strategies. *Int. J. Mol. Sci.* **2022**, *23*, 13283. [CrossRef]

71. Kumari, M.; Chaudhary, G.R.; Chaudhary, S.; Umar, A.; Akbar, S.; Baskoutas, S. Bio-Derived Fluorescent Carbon Dots: Synthesis, Properties and Applications. *Molecules* **2022**, *27*, 5329. [CrossRef]

72. Yao, L.; Zhao, M.-M.; Luo, Q.-W.; Zhang, Y.-C.; Liu, T.-T.; Yang, Z.; Liao, M.; Tu, P.; Zeng, K.-W. Carbon Quantum Dots-Based Nanozyme from Coffee Induces Cancer Cell Ferroptosis to Activate Antitumor Immunity. *ACS Nano* **2022**, *16*, 9228–9239. [CrossRef]

73. Zhang, B.; Liu, C.; Liu, Y. A Novel One-Step Approach to Synthesize Fluorescent Carbon Nanoparticles. *Eur. J. Inorg. Chem.* **2010**, *2010*, 4411–4414. [CrossRef]

74. Castañeda-Serna, H.U.; Calderón-Domínguez, G.; García-Bórquez, A.; Salgado-Cruz, M.d.l.P.; Rebollo, R.R.F. Structural and luminescent properties of CQDs produced by microwave and conventional hy-drothermal methods using pelagic Sargassum as carbon source. *Opt. Mater.* **2022**, *126*, 112156. [CrossRef]

75. Hong, Y.; Chen, X.; Zhang, Y.; Zhu, Y.; Sun, J.; Swihart, M.T.; Tan, K.; Dong, L. One-pot hydrothermal synthesis of high quantum yield orange-emitting carbon quantum dots for sensitive detection of per-fluorinated compounds. *New J. Chem.* **2022**, *41*, 19658–19666. [CrossRef]

76. Ye, H.; Liu, B.; Wang, J.; Zhou, C.; Xiong, Z.; Zhao, L. A Hydrothermal Method to Generate Carbon Quantum Dots from Waste Bones and Their Detection of Laundry Powder. *Molecules* **2022**, *27*, 6479. [CrossRef]

77. Huo, X.; Liu, L.; Bai, Y.; Qin, J.; Yuan, L.; Feng, F. Facile synthesis of yellowish-green emitting carbon quantum dots and their applications for phoxim sensing and cellular imaging. *Anal. Chim. Acta* **2021**, *1206*, 338685. [CrossRef]

78. Liu, H.; Ye, T.; Mao, C. Fluorescent Carbon Nanoparticles Derived from Candle Soot. *Angew. Chem.* **2007**, *119*, 6593–6595. [CrossRef]

79. Liu, R.; Wu, D.; Liu, S.; Koynov, K.; Knoll, W.; Li, Q. An Aqueous Route to Multicolor Photoluminescent Carbon Dots Using Silica Spheres as Carriers. *Angew. Chem. Int. Ed.* **2009**, *48*, 4598–4601. [CrossRef]

80. Pan, D.; Zhang, J.; Li, Z.; Wu, C.; Yan, X.; Wu, M. Observation of pH-, solvent-, spin-, and excitation-dependent blue photoluminescence from carbon nanoparticles. *Chem. Commun.* **2010**, *46*, 3681–3683. [CrossRef]

81. Martindale, B.C.M.; Hutton, G.A.M.; Caputo, C.A.; Reisner, E. Solar Hydrogen Production Using Carbon Quantum Dots and a Molecular Nickel Catalyst. *J. Am. Chem. Soc.* **2015**, *137*, 6018–6025. [CrossRef] [PubMed]

82. Rong, M.; Feng, Y.; Wang, Y.; Chen, X. One-pot solid phase pyrolysis synthesis of nitrogen-doped carbon dots for Fe3+ sensing and bioimaging. *Sens. Actuators B Chem.* **2017**, *245*, 868–874. [CrossRef]

83. Ma, C.; Zhou, Y.; Yan, W.; He, W.; Liu, Q.; Li, Z.; Wang, H.; Li, X. Predominant catalytic performance of nickel nanoparticles embedded into nitrogen-doped carbon quantum dot-based nanosheets for the nitrore-duction of halogenated nitrobenzene. *ACS Sustain. Chem. Eng.* **2022**, *25*, 8162–8171. [CrossRef]

84. Otten, M.; Hildebrandt, M.; Kühnemuth, R.; Karg, M. Pyrolysis and Solvothermal Synthesis for Carbon Dots: Role of Purification and Molecular Fluorophores. *Langmuir* **2022**, *38*, 6148–6157. [CrossRef] [PubMed]

85. Krishnamoorthy, K.; Veerapandian, M.; Mohan, R.; Kim, S.-J. Investigation of Raman and photoluminescence studies of reduced graphene oxide sheets. *Appl. Phys. A* **2011**, *106*, 501–506. [CrossRef]

86. Zong, J.; Zhu, Y.; Yang, X.; Shen, J.; Li, C. Synthesis of photoluminescent carbogenic dots using mesoporous silica spheres as nanoreactors. *Chem. Commun.* **2010**, *47*, 764–766. [CrossRef]

87. Ahlawat, A.; Rana, P.S.; Solanki, P.R. Studies of photocatalytic and optoelectronic properties of microwave synthesized and polyethyleneimine stabilized carbon quantum dots. *Mater. Lett.* **2021**, *305*, 130830. [CrossRef]

88. Architha, N.; Ragupathi, M.; Shobana, C.; Selvankumar, T.; Kumar, P.; Lee, Y.S.; Selvan, R.K. Microwave-assisted green synthesis of fluorescent carbon quantum dots from Mexican Mint extract for Fe3+ detection and bio-imaging applications. *Environ. Res.* **2021**, *199*, 111263. [CrossRef]

89. Harshita, L.; Yadav, P.; Jain, Y.; Sharma, M.; Reza, M.; Agarwal, M.; Gupta, R. One-pot microwave-assisted synthesis of blue emissive multifunctional NSP co-doped carbon dots as a nanoprobe for sequential detection of Cr (VI) and ascorbic acid in real samples, fluorescent ink and logic gate operation. *J. Mol. Liq.* **2022**, *346*, 117088.

90. Larsson, M.A.; Ramachandran, P.; Jarujamrus, P.; Lee, H.L. Microwave Synthesis of Blue Emissive N-Doped Carbon Quantum Dots as a Fluorescent Probe for Free Chlorine Detection. *Sains Malays.* **2022**, *51*, 1197–1212. [CrossRef]

91. Jeong, G.; Lee, J.M.; Lee, J.a.; Praneerad, J.; Choi, C.A.; Supchocksoonthorn, P.; Roy, A.K.; In, I. Microwave-assisted synthesis of multifunctional fluorescent carbon quantum dots from A4/B2 polyamidation monomer sets. *Appl. Surf. Sci.* **2021**, *542*, 148471. [CrossRef]

92. Bourlinos, A.B.; Stassinopoulos, A.; Anglos, D.; Zboril, R.; Georgakilas, V.; Giannelis, E.P. Photoluminescent Carbogenic Dots. *Chem. Mater.* **2008**, *20*, 4539–4541. [CrossRef]

93. Tang, L.; Ji, R.; Cao, X.; Lin, J.; Jiang, H.; Li, X.; Teng, K.S.; Luk, C.M.; Zeng, S.; Hao, J.; et al. Deep Ultraviolet Photoluminescence of Water-Soluble Self-Passivated Graphene Quantum Dots. *ACS Nano* **2012**, *6*, 5102–5110. [CrossRef]

94. Hola, K.; Bourlinos, A.B.; Kozak, O.; Berka, K.; Siskova, K.M.; Havrdova, M.; Tucek, J.; Safarova, K.; Otyepka, M.; Giannelis, E.P.; et al. Photoluminescence effects of graphitic core size and surface functional groups in carbon dots: COO− induced red-shift emission. *Carbon* **2014**, *70*, 279–286. [CrossRef]

95. Sciortino, A.; Marino, E.; van Dam, B.; Schall, P.; Cannas, M.; Messina, F. Solvatochromism un-ravels the emission mechanism of carbon nanodots. *J. Phys. Chem. Lett.* **2016**, *17*, 3419–3423. [CrossRef]

96. Dager, A.; Uchida, T.; Maekawa, T.; Tachibana, M. Synthesis and characterization of Mono-disperse Carbon Quantum Dots from Fennel Seeds: Photoluminescence analysis using Machine Learning. *Sci. Rep.* **2019**, *9*, 14004. [CrossRef]

97. Zhang, W.; Yu, S.F.; Fei, L.; Jin, L.; Pan, S.; Lin, P. Large-area color controllable remote carbon white-light light-emitting diodes. *Carbon* **2015**, *85*, 344–350. [CrossRef]

98. Martindale, B.C.M.; Hutton, G.A.M.; Caputo, C.A.; Prantl, S.; Godin, R.; Durrant, J.R.; Reisner, E. Enhancing Light Absorption and Charge Transfer Efficiency in Carbon Dots through Graphitization and Core Nitrogen Doping. *Angew. Chem.* **2017**, *129*, 6559–6563. [CrossRef]

99. Tingting, Y.; Wang, H.; Guo, C.; Zhai, Y.; Yang, J.; Yuan, J. A rapid microwave synthesis of green-emissive carbon dots with solid-state fluorescence and pH-sensitive properties. *R. Soc. Open Sci.* **2018**, *7*, 180245.

100. Haitao, L.; Kang, Z.; Liu, Y.; Lee, S.-T. Carbon nanodots: Synthesis, properties and applications. *J. Mater. Chem.* **2012**, *46*, 24230–24253.

101. Zheng, Y.; Yang, D.; Wu, X.; Yan, H.; Zhao, Y.; Feng, B.; Duan, K.; Weng, J.; Wang, J. A facile approach for the synthesis of highly luminescent carbon dots using vitamin-based small organic molecules with benzene ring structure as precursors. *RSC Adv.* **2015**, *5*, 90245–90254. [CrossRef]

102. Hou, H.; Banks, C.E.; Jing, M.; Zhang, Y.; Ji, X. Carbon Quantum Dots and Their Derivative 3D Porous Carbon Frameworks for Sodium-Ion Batteries with Ultralong Cycle Life. *Adv. Mater.* **2015**, *27*, 7861–7866. [CrossRef]

103. Semeniuk, M.; Yi, Z.; Poursorkhabi, V.; Tjong, J.; Jaffer, S.; Lu, Z.-H.; Sain, M. Future per-spectives and review on organic carbon dots in electronic applications. *ACS Nano* **2019**, *6*, 6224–6255. [CrossRef] [PubMed]

104. Bomben, K.D.; Moulder, J.F.; Stickle, W.F.; Sobol, P.E. *Handbook of X-Ray Photoelectron Spectroscopy: A Reference Book of Standard Spectra for Identication and Interpretation of XPS, Physical Electronics, Eden Prairie*; Perkin-Elmer Corporation: Waltham, MA, USA, 1995.

105. Zhou, Y.; Sharma, S.K.; Peng, Z.; Leblanc, R.M. Polymers in Carbon Dots: A Review. *Polymers* **2017**, *9*, 67. [CrossRef] [PubMed]

106. Kolanowska, A.; Dzido, G.; Krzywiecki, M.; Tomczyk, M.M.; Łukowiec, D.; Ruczka, S.; Boncel, S. Carbon Quantum Dots from Amino Acids Revisited: Survey of Renewable Precursors toward High Quan-tum-Yield Blue and Green Fluorescence. *ACS Omega* **2022**, *45*, 41165–41176. [CrossRef]

107. Qiang, S.; Zhang, L.; Li, Z.; Liang, J.; Li, P.; Song, J.; Guo, K.; Wang, Z.; Fan, Q. New Insights into the Cellular Toxicity of Carbon Quantum Dots to *Escherichia coli*. *Antioxidants* **2022**, *11*, 2475. [CrossRef]

108. Gayen, B.; Palchoudhury, S.; Chowdhury, J. Carbon Dots: A Mystic Star in the World of Nanoscience. *J. Nanomater.* **2019**, 1–19. [CrossRef]

109. Hu, C.; Yu, C.; Li, M.; Wang, X.; Yang, J.; Zhao, Z.; Eychmüller, A.; Sun, Y.-P.; Qiu, J. Chemically Tailoring Coal to Fluorescent Carbon Dots with Tuned Size and Their Capacity for Cu(II) Detection. *Small* **2014**, *10*, 4926–4933. [CrossRef]

110. Wang, S.; Kirillova, K.; Lehto, X. Travelers' food experience sharing on social network sites. *J. Travel Tour. Mark.* **2016**, *34*, 680–693. [CrossRef]

111. Jiang, K.; Zhang, L.; Lu, J.; Xu, C.; Cai, C.; Lin, H. Triple-Mode Emission of Carbon Dots: Applications for Advanced Anti-Counterfeiting. *Angew. Chem.* **2016**, *128*, 7347–7351. [CrossRef]

112. Li, F.; Li, Y.; Yang, X.; Han, X.; Jiao, Y.; Wei, T.; Yang, D.; Xu, H.; Nie, G. Highly Fluorescent Chiral N-S-Doped Carbon Dots from Cysteine: Affecting Cellular Energy Metabolism. *Angew. Chem.* **2018**, *130*, 2401–2406. [CrossRef]

113. Anwar, S.; Ding, H.; Xu, M.; Hu, X.; Li, Z.; Wang, J.; Bi, H. Recent advances in synthesis, optical properties, and bio-medical applications of carbon dots. *ACS Appl. Bio Mater.* **2019**, *6*, 2317–2338. [CrossRef]

114. Jhonsi, M.A. Carbon Quantum Dots for Bioimaging. In *State of the Art in Nano-Bioimaging*; IntechOpen: London, UK, 2018; pp. 35–55.

115. Konstantinos, D. Carbon quantum dots: Surface passivation and functionalization. *Curr. Org. Chem.* **2016**, *6*, 682–695.

116. Li, L.; Dong, T. Photoluminescence tuning in carbon dots: Surface passivation or/and functionalization, heteroatom doping. *J. Mater. Chem. C* **2018**, *30*, 7944–7970. [CrossRef]

117. Peng, H.; Travas-Sejdic, J. Simple Aqueous Solution Route to Luminescent Carbogenic Dots from Carbohydrates. *Chem. Mater.* **2009**, *21*, 5563–5565. [CrossRef]

118. Wang, L.; Li, W.; Yin, L.; Liu, Y.; Guo, H.; Lai, J.; Han, Y.; Li, G.; Li, M.; Zhang, J.; et al. Full-color fluorescent carbon quantum dots. *Sci. Adv.* **2020**, *6*, eabb6772. [CrossRef]

119. Nisha, P.; Amrita, D. Theoretical study of Dependence of Wavelength on Size of Quantum Dot. *Int. J. Sci. Res. Dev.* **2016**, *4*, 126–130.

120. Kandasamy, G. Recent Advancements in Doped/Co-Doped Carbon Quantum Dots for Multi-Potential Applications. *C* **2019**, *5*, 24. [CrossRef]

121. Darragh, C.; Rocks, C.; Padmanaban, D.B.; Maguire, P.; Svrcek, V.; Mariotti, D. Environmentally friendly nitrogen-doped carbon quantum dots for next generation solar cells. *Sustain. Energy Fuels* **2017**, *7*, 1611–1619.

122. Gao, R.; Wu, Z.; Wang, L.; Liu, J.; Deng, Y.; Xiao, Z.; Fang, J.; Liang, Y. Green Preparation of Fluorescent Nitrogen-Doped Carbon Quantum Dots for Sensitive Detection of Oxytetracycline in Environmental Samples. *Nanomaterials* **2020**, *10*, 1561. [CrossRef]

123. Yu, J.; Liu, C.; Yuan, K.; Lu, Z.; Cheng, Y.; Li, L.; Zhang, X.; Jin, P.; Meng, F.; Liu, H. Luminescence Mechanism of Carbon Dots by Tailoring Functional Groups for Sensing Fe3+ Ions. *Nanomaterials* **2018**, *8*, 233. [CrossRef] [PubMed]

124. Zuo, G.; Xie, A.; Li, J.; Su, T.; Pan, X.; Dong, W. Large Emission Red-Shift of Carbon Dots by Fluorine Doping and Their Applications for Red Cell Imaging and Sensitive Intracellular Ag$^+$ Detection. *J. Phys. Chem. C* **2017**, *121*, 26558–26565. [CrossRef]

125. Baker, S.N.; Baker, G.A. Luminescent carbon nanodots: Emergent nanolights. *Angew. Chem. Int. Ed.* **2010**, *49*, 6726–6744. [CrossRef] [PubMed]

126. Gokus, T.; Nair, R.R.; Bonetti, A.; Böhmler, M.; Lombardo, A.; Novoselov, K.; Geim, A.K.; Ferrari, A.C.; Hartschuh, A. Making Graphene Luminescent by Oxygen Plasma Treatment. *ACS Nano* **2009**, *3*, 3963–3968. [CrossRef]

127. Demchenko, A.P.; Dekaliuk, M.O. Novel fluorescent carbonic nanomaterials for sensing and imaging. *Methods Appl. Fluoresc.* **2013**, *1*, 042001. [CrossRef]

128. Zhang, Q.; Wang, R.; Feng, B.; Zhong, X.; Ostrikov, K. Photoluminescence mechanism of carbon dots: Triggering high-color-purity red fluorescence emission through edge amino protonation. *Nat. Commun.* **2021**, *12*, 6856. [CrossRef]

129. Nguyen, H.A.; Srivastava, I.; Pan, D.; Gruebele, M. Unraveling the Fluorescence Mechanism of Carbon Dots with *Sub*-Single-Particle Resolution. *ACS Nano* **2020**, *14*, 6127–6137. [CrossRef]

130. An, Y.; Liu, C.; Li, Y.; Chen, M.; Zheng, Y.; Tian, H.; Shi, R.; He, X.; Lin, X. Preparation of Multicolour Solid Fluorescent Carbon Dots for Light-Emitting Diodes Using Phenylethylamine as a Co-Carbonization Agent. *Int. J. Mol. Sci.* **2022**, *23*, 11071. [CrossRef]

131. Cao, L.; Meziani, M.J.; Sahu, S.; Sun, Y.-P. Photoluminescence Properties of Graphene versus Other Carbon Nanomaterials. *Acc. Chem. Res.* **2012**, *46*, 171–180. [CrossRef]

132. Fang, Y.; Guo, S.; Li, D.; Zhu, C.; Ren, W.; Dong, S.; Wang, E. Easy Synthesis and Imaging Applications of Cross-Linked Green Fluorescent Hollow Carbon Nanoparticles. *ACS Nano* **2011**, *6*, 400–409. [CrossRef]

133. Shen, J.; Zhu, Y.; Chen, C.; Yang, X.; Li, C. Facile preparation and upconversionlumi-nescence of graphene quantum dots. *Chem. Commun.* **2011**, *9*, 2580–2582. [CrossRef]

134. Li, X.; Wang, H.; Shimizu, Y.; Pyatenko, A.; Kawaguchi, K.; Koshizaki, N. Preparation of carbon quantum dots with tunable photoluminescence by rapid laser passivation in ordinary organic solvents. *Chem. Commun.* **2010**, *47*, 932–934. [CrossRef]

135. Nourbakhsh, A.; Cantoro, M.; Vosch, T.; Pourtois, G.; Clemente, F.; van der Veen, M.; Hofkens, J.; Heyns, M.M.; De Gendt, S.; Sels, B.F. Bandgap opening in oxygen plasma-treated graphene. *Nanotechnology* **2010**, *21*, 435203. [CrossRef]

136. Dekaliuk, M.O.; Viagin, O.; Malyukin, Y.V.; Demchenko, A.P. Fluorescent carbon nanomateri-als:"Quantum dots" or nanoclusters? *Phys. Chem. Chem. Phys.* **2014**, *30*, 16075–16084. [CrossRef]

137. Bibekananda, D.; Karak, N. A green and facile approach for the synthesis of water soluble fluorescent carbon dots from banana juice. *RSC Adv.* **2013**, *22*, 8286–8290.

138. Dong, Y.; Shao, J.; Chen, C.; Li, H.; Wang, R.; Chi, Y.; Lin, X.; Chen, G. Blue luminescent graphene quantum dots and graphene oxide prepared by tuning the carbonization degree of citric acid. *Carbon* **2012**, *50*, 4738–4743. [CrossRef]

139. Zhi, B.; Yao, X.; Cui, Y.; Orr, G.; Haynes, C.L. Synthesis, applications and potential photoluminescence mechanism of spectrally tunable carbon dots. *Nanoscale* **2019**, *11*, 20411–20428. [CrossRef]

140. De Caluwé, E.; Halamouá, K.; Van Damme, P.; Adansoniadigitata, L. A review of traditional uses, phytochemistry and pharmacology. *Afr. Focus* **2010**, *1*, 11–51. [CrossRef]

141. Lu, C.; Su, Q.; Yang, X. Ultra-long room-temperature phosphorescent carbon dots: pH sensing and dual-channel detection of tetracyclines. *Nanoscale* **2019**, *11*, 16036–16042. [CrossRef]

142. Gao, W.; Zhang, S.; Wang, G.; Cui, J.; Lu, Y.; Rong, X.; Gao, C. A review on mechanism, applications and influencing factors of carbon quantum dots based photocatalysis. *Ceram. Int.* **2022**, *48*, 35986–35999. [CrossRef]

143. Das, R.; Bandyopadhyay, R.; Pramanik, P. Carbon quantum dots from natural resource: A review. *Mater. Today Chem.* **2018**, *8*, 96–109. [CrossRef]

144. Xu, J.; Tao, J.; Su, L.; Wang, J.; Jiao, T. A Critical Review of Carbon Quantum Dots: From Synthesis toward Applications in Electrochemical Biosensors for the Determination of a Depression-Related Neurotransmitter. *Materials* **2021**, *14*, 3987. [CrossRef]

145. Dong, Y.-L.; Zhang, H.-G.; Rahman, Z.U.; Su, L.; Chen, X.-J.; Hu, J.; Chen, X.-G. Graphene oxide−Fe3O4 magnetic nanocomposites with peroxidase-like activity for colorimetric detection of glucose. *Nanoscale* **2012**, *4*, 3969–3976. [CrossRef]

146. Ryan, B.J.; Carolan, N.; Ó'Fágáin, C. Horseradish and soybean peroxidases: Comparable tools for alternative niches? *Trends Biotechnol.* **2006**, *24*, 355–363. [CrossRef] [PubMed]

147. Gao, L.; Zhuang, J.; Nie, L.; Zhang, J.; Zhang, Y.; Gu, N.; Wang, T.; Feng, J.; Yang, D.; Perrett, S.; et al. Intrinsic peroxidase-like activity of ferromagnetic nanoparticles. *Nat. Nanotechnol.* **2007**, *2*, 577–583. [CrossRef] [PubMed]

148. Floss, M.A.; Fink, T.; Maurer, F.; Volk, T.; Kreuer, S.; Müller-Wirtz, L.M. Exhaled Aldehydes as Biomarkers for Lung Diseases: A Narrative Review. *Molecules* **2022**, *27*, 5258. [CrossRef]

149. Li, J.; Yao, S.-L.; Liu, S.-J.; Chen, Y.-Q. Fluorescent sensors for aldehydes based on luminescent metal–organic frameworks. *Dalton Trans.* **2021**, *50*, 7166–7175. [CrossRef]

150. Ibáñez, D.; González-García, M.B.; Hernández-Santos, D.; Fanjul-Bolado, P. Spectroelectrochemical Enzyme Sensor System for Acetaldehyde Detection in Wine. *Biosensors* **2022**, *12*, 1032. [CrossRef]

151. Mohammadi, M.; Khazaei, A.; Rezaei, A.; Huajun, Z.; Xuwei, S. Ionic-Liquid-Modified Carbon Quantum Dots as a Support for the Immobilization of Tungstate Ions (WO_4^{2-}): Heterogeneous Nanocatalysts for the Oxidation of Alcohols in Water. *ACS Sustain. Chem. Eng.* **2019**, *7*, 5283–5291. [CrossRef]

152. Mahamuni, N.N.; Gogate, P.R.; Pandit, A.B. Selective synthesis of sulfoxides from sulfides using ultrasound. *Ultrason. Sonochem.* **2007**, *2*, 135–142. [CrossRef] [PubMed]

153. An, H.; Luo, H.; Xu, T.; Chang, S.; Chen, Y.; Zhu, Q.; Huang, Y.; Tan, H.; Li, Y.-G. Visible-Light-Driven Oxidation of Amines to Imines in Air Catalyzed by Polyoxometalate–Tris(bipyridine)ruthenium Hybrid Compounds. *Inorg. Chem.* **2022**, *61*, 10442–10453. [CrossRef]

154. Chen, W.; Li, H.; Song, J.; Zhao, Y.; Ma, P.; Niu, J.; Wang, J. Binuclear Ru(III)-Containing Polyoxometalate with Efficient Photocatalytic Activity for Oxidative Coupling of Amines to Imines. *Inorg. Chem.* **2022**, *61*, 2076–2085. [CrossRef] [PubMed]

155. Kawahara, N.; Palasin, K.; Asano, Y. Novel Enzymatic Method for Imine Synthesis via the Oxi-dation of Primary Amines Using D-Amino Acid Oxidase from Porcine Kidney. *Catalysts* **2022**, *5*, 511. [CrossRef]

156. Pyun, J. Graphene oxide as catalyst: Application of carbon materials beyond nanotechnology. *Angew. Chem. Int. Ed.* **2011**, *1*, 46–48. [CrossRef]

157. Su, D.S.; Zhang, J.; Frank, B.; Thomas, A.; Wang, X.; Paraknowitsch, J.; Schlögl, R. Metal-Free Heterogeneous Catalysis for Sustainable Chemistry. *Chemsuschem* **2010**, *3*, 169–180. [CrossRef]

158. Yu, H.; Peng, F.; Tan, J.; Hu, X.; Wang, H.; Yang, J.; Zheng, W. Selective Catalysis of the Aerobic Oxidation of Cyclohexane in the Liquid Phase by Carbon Nanotubes. *Angew. Chem.* **2011**, *123*, 4064–4068. [CrossRef]

159. Shiri, M. Indoles in Multicomponent Processes (MCPs). *Chem. Rev.* **2012**, *112*, 3508–3549. [CrossRef]

160. Vidhya, L.N.; Thirumurugan, P.; Noorulla, K.M.; Perumal, P.T. InCl3 mediated one-pot multicomponent synthesis, anti-microbial, antioxidant and anticancer evaluation of 3-pyranyl indole derivatives. *Bioorganic Med. Chem. Lett.* **2010**, *17*, 5054–5061.

161. Gomha, S.M.; Abdel-Aziz, H.A. Synthesis of new heterocycles derived from 3-(3-methyl-1H-indol-2-yl)-3-oxopropanenitrile as potent antifungal agents. *Bull. Korean Chem. Soc.* **2012**, *9*, 2985–2990. [CrossRef]

162. Fadda, A.A.; El-Mekabaty, A.; Mousa, I.A.; Elattar, K.M. Chemistry of 3-(1H-Indol-3-yl)-3-oxopropanenitrile. *Synth. Commun.* **2014**, *44*, 1579–1599. [CrossRef]

163. Thirumurugan, P.; Nandakumar, A.; Muralidharan, D.; Perumal, P.T. Simple and convenient approach to the Kr€ ohnke pyridine type synthesis of functionalized indol-3-yl pyridine derivatives using 3-cyanoacetyl indole. *J. Comb. Chem.* **2010**, *1*, 161–167. [CrossRef] [PubMed]

164. Irfan, S.M.; Khan, P.; Abid, M.; Khan, M.M. Design, synthesis, and biological evaluation of novel fused spiro-4 H-pyran derivatives as bacterial biofilm disruptor. *ACS Omega* **2019**, *16*, 16794–16807.

165. Kumar, S.P.; Silakari, O. The current status of O-heterocycles: A synthetic and medicinal overview. *ChemMedChem* **2018**, *11*, 1071–1087.

166. Zhao, L.; Sun, Z.; Ma, J. Novel Relationship between Hydroxyl Radical Initiation and Surface Group of Ceramic Honeycomb Supported Metals for the Catalytic Ozonation of Nitrobenzene in Aqueous Solution. *Environ. Sci. Technol.* **2009**, *43*, 4157–4163. [CrossRef]

167. McKeen, J.C.; Yan, Y.S.; Davis, M.E. Proton Conductivity in Sulfonic Acid-Functionalized Zeolite Beta: Effect of Hydroxyl Group. *Chem. Mater.* **2008**, *20*, 3791–3793. [CrossRef]

168. Doyle, A.G.; Jacobsen, E.N. Small-molecule H-bond donors in asymmetric catalysis. *Chem. Rev.* **2007**, *12*, 5713–5743. [CrossRef]

169. Chen, X.; Brauman, J.I. Hydrogen bonding lowers intrinsic nucleophilicity of solvated nucleophiles. *J. Am. Chem. Soc.* **2008**, *45*, 15038–15046. [CrossRef]

170. Kitano, M.; Nakajima, K.; Kondo, J.N.; Hayashi, S.; Hara, M. Protonated Titanate Nanotubes as Solid Acid Catalyst. *J. Am. Chem. Soc.* **2010**, *132*, 6622–6623. [CrossRef]

171. Navalon, S.; Dhakshinamoorthy, A.; Alvaro, M.; Garcia, H. Carbocatalysis by graphene-based materials. *Chem. Rev.* **2014**, *12*, 6179–6212. [CrossRef]

172. Chang, B.; Fu, J.; Tian, Y.; Dong, X. Multifunctionalized Ordered Mesoporous Carbon as an Efficient and Stable Solid Acid Catalyst for Biodiesel Preparation. *J. Phys. Chem. C* **2013**, *117*, 6252–6258. [CrossRef]

173. Fekry, A.M. An Innovative Simple Electrochemical Levofloxacin Sensor Assembled from Carbon Paste Enhanced with Nano-Sized Fumed Silica. *Biosensors* **2022**, *12*, 906. [CrossRef] [PubMed]

174. Sitara, E.; Ehsan, M.F.; Nasir, H.; Iram, M.; Bukhari, A.B. Synthesis, characterization and photocatalytic activity of MoS2/ZnSe heterostructures for the degradation of levofloxacin. *Catalysts* **2020**, *12*, 1380. [CrossRef]